Accepted Manuscript

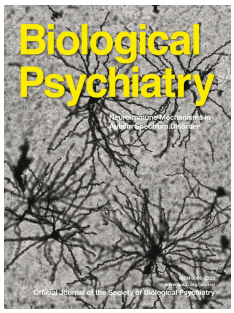

Common Dysfunction of Large-Scale Neurocognitive Networks across Psychiatric Disorders

Zhiqiang Sha, Tor D. Wager, Andrea Mechelli, Yong He

PII: S0006-3223(18)32023-7

DOI: https://doi.org/10.1016/j.biopsych.2018.11.011

Reference: BPS 13693

To appear in: *Biological Psychiatry*

Received Date: 22 June 2018

Revised Date: 8 November 2018

Please cite this article as: Sha Z., Wager T.D., Mechelli A. & He Y., Common Dysfunction of Large-Scale Neurocognitive Networks across Psychiatric Disorders, *Biological Psychiatry* (2018), doi: https://doi.org/10.1016/j.biopsych.2018.11.011.

Common Dysfunction of Large-Scale Neurocognitive Networks across Psychiatric Disorders

Zhiqiang Sha[1,2,3]; Tor D. Wager [4,5]; Andrea Mechelli [6]; Yong He [1,2,3*]

[1] National Key Laboratory of Cognitive Neuroscience and Learning, Beijing Normal University, Beijing, 100875, China

[2] Beijing Key Laboratory of Brain Imaging and Connectomics, Beijing Normal University, Beijing, 100875, China

[3] IDG/McGovern Institute for Brain Research, Beijing Normal University, Beijing, 100875, China

[4] Department of Psychology and Neuroscience, Muezinger D244, 345 UCB, Boulder, Colorado 80309-0345, USA

[5] Institute of Cognitive Science, University of Colorado, 344 UCB, Boulder, Colorado 80309-0344, USA

[6] Department of Psychosis Studies, Institute of Psychiatry, Psychology & Neuroscience, King's College London, London SE5 8AF, UK

Running Title: Disrupted cognitive networks across psychopathology

*__Corresponding author__:

Yong He, Ph.D., National Key Laboratory of Cognitive Neuroscience and Learning, IDG/McGovern Institute for Brain Research, Beijing Key Laboratory of Brain Imaging and Connectomics, Beijing Normal University, China; Tel/Fax: 8610-5880-2036; E-mail: yong.he@bnu.edu.cn

Manuscript information: 27 text pages, 4 figures, 1 table, 4000 words.

(Supplementary Information: 28 text pages, 11 figures, 8 tables.)

Abstract

BACKGROUND: Cognitive dysfunction is one of the most prominent characteristics of psychiatric disorders. At present, the neural correlates of cognitive dysfunction across psychiatric disorders are poorly understood. The aim of this study was to investigate functional connectivity and structural perturbations across psychiatric diagnoses in three neurocognitive networks of interest, including the default-mode (DMN), the frontoparietal (FPN) and the salience network (SN).

METHODS: We performed meta-analyses of resting-state functional MRI (R-fMRI) whole-brain seed-based functional connectivity in 8,298 patients (involving 8 disorders) and 8,165 healthy controls and a voxel-based morphometry analysis of structural MRI data in 14,027 patients (involving 8 disorders) and healthy 14,504 controls. To aid the interpretation of the results, we examined neurocognitive function in 776 healthy participants from the Human Connectome Project.

RESULTS: We found that the three neurocognitive networks of interest were characterized by shared alterations of functional connectivity architecture across psychiatric disorders. More specifically, hypoconnectivity was expressed between the DMN and ventral SN and between the SN and FPN, whereas hyperconnectivity was evident between the DMN and FPN and between the DMN and dorsal SN. This pattern of network alterations was associated with gray matter reductions in patients, and was localized in regions that subserve general cognitive performance.

CONCLUSIONS: This study is the first to provide meta-analytic evidence of common alterations of functional connectivity within and between neurocognitive networks. The findings suggest a shared mechanism of network interactions that may associate with the generalized cognitive deficits observed in psychiatric disorders.

Keywords: connectomics, default-mode network, frontoparietal network, salience network, meta-analysis, resting-state fMRI

Introduction

Contemporary psychiatry is rooted in the notion that psychiatric disorders are distinct, independent categories with unique clinical presentations. However, in everyday clinical practice, psychiatric disorders tend to have heterogeneous clinical presentations with high co-occurrence (1-3). A common feature of multiple psychiatric disorders is the presence of cognitive deficits, particularly in executive control, working memory and salience processing (4-6). Moreover, the presence of cognitive dysfunction has been found to have common neurobiological correlates in the dorsolateral prefrontal cortex (dlPFC), insula and dorsal anterior cingulate cortex (dACC) across different psychiatric disorders (7, 8). Collectively, these findings suggest that cognitive impairment may be a trans-diagnostic feature of psychiatric disorders (9). Such cognitive dysfunction cannot be explained by localized changes in a small number of regions (10-12); instead, this dysfunction appears to arise from functional alterations within and between large-scale neural networks, consistent with the notion of psychiatric disorders as "disconnection syndromes". Thus, studying the pathoconnectome associated with cognitive deficits across multiple psychiatric disorders may allow the identification of transdiagnostic neurobiological mechanisms that underlie multiple forms of psychopathology (13-15).

Among the functional networks identified in the human brain, Menon proposed the existence of three "core" neurocognitive networks that may be affected in multiple psychiatric disorders: the default-mode network (DMN), the frontoparietal network (FPN) and the salience network (SN) (16). The DMN, which is mainly composed of the medial PFC (mPFC), posterior cingulate cortex (PCC) and lateral temporal cortex, supports internally oriented attention and self-monitoring, among other functions (17). The FPN, including the dlPFC, dorsomedial PFC (dmPFC) and dorsolateral parietal cortex, is implicated in executive control (18, 19). Finally, the SN, consisting of the dACC, insula and caudate, is involved in orienting toward salient external stimuli and internal events (16, 20). A number of recent

studies have demonstrated that functional connectivity within and between these neurocognitive networks is closely related to cognitive deficits in most psychiatric disorders (15, 21, 22).

Currently, however, our understanding of the pathoconnectomics of cognitive dysfunction across psychiatric disorders is hampered by several limitations in the existing literature, such as small sample sizes, inconsistent recruitment criteria and heterogeneous results. Meta-analyses can be used to test for homogeneous and reliable patterns in the existing literature (23, 24). Our recent meta-connectomic analysis across 182 whole-brain resting-state fMRI (R-fMRI) studies, which included 13,375 individuals (6,683 patients/6,692 healthy controls), revealed several regions, including the ventromedial PFC, dlPFC and motor cortex, with functional alterations across disorders (25). However, this meta-analysis did not consider the functional connectivity between large-scale neurocognitive networks, and was therefore unable to reveal the neural basis of trans-diagnostic cognitive dysfunction. In addition, this meta-analysis utilized R-fMRI data without considering possible alterations in gray matter volume. Therefore, whether functional architecture between large-scale neurocognitive networks across disorders is associated with structural perturbations remains unclear. Collectively, the identification of multi-modal alterations of large-scale neurocognitive networks across disorders could help elucidate trans-diagnostic functional and structural mechanisms underlying cognitive dysfunction.

To address these issues, we conducted whole-brain meta-analyses of 242 R-fMRI and 363 structural MRI studies to examine multi-modal alterations of large-scale neurocognitive networks across psychiatric diagnoses, followed by graph-based analysis of R-fMRI data in 766 healthy subjects to explore the cognitive function of network connectivity. First, we hypothesized altered functional connectivity within and between the three neurocognitive networks of interest across psychiatric disorders. Second, we hypothesized multi-modal disruption of these neurocognitive networks, with regions showing functional alterations also showing gray matter loss. Third, functional connectivity

alterations across psychiatric disorders would be localized in regions that subserve distinct aspects of cognitive performance in healthy participants.

Material and Methods

Dataset Overview

This study included 3 large datasets (Table 1). Dataset 1, which comprised 242 whole-brain seed-based functional connectivity (SB-FC) R-fMRI studies, was used to detect common network alterations across psychiatric disorders. Dataset 2, which included studies of 363 whole-brain VBM analyses with structural MRI data, was used to test for gray matter volumetric changes across psychiatric disorders. Dataset 3, which included R-fMRI data from 766 healthy participants from the Human Connectome Project, was used to determine whether these network connectivity identified in patients were associated with cognitive performance on behavioral tests.

SB-FC Meta-Analysis (Dataset 1)

Study Selection

A step-wise procedure was used to search the relevant studies by adopting the "Preferred Reporting Items for Systematic Reviews and Meta-Analyses" (PRISMA) guidelines (http://www.prisma-statement.org/). Studies published in English before February 2017 were identified by searching five online public datasets, including PubMed (PubMed Central), Neurosynth, ScienceDirect, Web of Science and the BrainMap database. Studies including patients with Axis I psychiatric diagnoses were selected for further analysis. The selected studies were restricted to whole-brain R-fMRI studies using voxel-wise SB-FC to compare differences between patients and healthy control groups (see Supplement). These criteria led to the inclusion of 242 SB-FC studies of 8 psychiatric disorders with 8,298 patients and 8,165 normal controls (Fig. S1, S2 and Table S1).

Data Extraction

To identify alterations in functional connectivity in case-control studies, we extracted information reflecting the locations of the seeds and the peak coordinates of significant between-group SB-FC differences, which reflect group-level differences between patients and healthy controls. Seeds were categorized into three seed networks defined by our previous voxel-wise modular detection (25), including the DMN, FPN and SN (Fig. 1A and details in Supplement). The effects of SB-FC were categorized into two groups: hypoconnectivity (Patients < Healthy Controls) and hyperconnectivity (Patients > Healthy Controls).

Multilevel Kernel Density Analysis (MKDA)

SB-FC meta-analysis (26, 27) was performed using the MKDA toolbox (http://wagerlab.colorado.edu). We first converted the coordinates reported in Talairach space to Montreal Neurological Institute standard space (26, 28). Then, peak coordinates for seed-network comparisons in each study were convolved with a proposed spherical kernel between 10 and 15mm (r = 15mm) (29) thresholded at a maximum value of 1, resulting in an indicator map (IM) for each study. We repeated this using another spherical kernel radius (r = 13mm) to assess the robustness of the findings. In each IM map, a value of 1 suggested a significant effect in the neighborhood, and a value of 0 indicated the absence of a peak in the local vicinity. Subsequently, a weighted average of all the IM maps was computed to assess the density of effects. We then performed Monte Carlo simulation (10,000 iterations) with the weighted average density maps to establish a familywise error (FWE) threshold for multiple comparisons. Density maps can be thresholded by two approaches: *height*-based (*hb*) and *extent*-based (*eb*) thresholding. The former indicates that the density at a given voxel is above the maximum expected over the whole brain by chance ($p < 0.05$), and the latter indicates that the density at that cluster exceeds the maximum expected in a cluster of a certain size by chance ($p < 0.001$) (see Supplement). In this study, we refer to

"within-network" and "between-network" alterations to indicate that the effects fall within or beyond the functional network where the seeds are located, respectively.

Post Hoc Analyses

Four kinds of post hoc analysis were performed to validate the outcomes of our meta-analysis. First, to test whether the results were affected by head motion (30, 31) and global signal (32, 33), we separately repeated the meta-analysis with studies that did and did not remove head movement or global signal, and compared the effect sizes for the different preprocessing strategies. Second, to assess whether the results were independent of the inclusion of a specific study, we performed a series of additional meta-analyses with leave-one-study-out ("jackknife") validation (34) (see Supplement). Third, to evaluate whether the results for the DMN network were biased by the fact that most of the studies focused on depressive disorder and schizophrenia and that altered patterns within the neurocognitive networks were frequently reported in both disorders (27, 35), we separately repeated the SB-FC meta-analysis of the DMN network after excluding studies on depression and schizophrenia. Finally, Fisher's exact test was used to investigate the moderation of effects by clinical and demographic factors, including comorbidity, medication status, age or gender (see Supplement).

VBM Meta-Analysis (Dataset 2)

Whole-brain VBM meta-analysis of structural imaging studies was used to determine the structural substrates of altered functional connectivity across psychiatric disorders. Consistent with the meta-analysis of SB-FC studies, a similar procedure was performed to select studies related to VBM analysis. A total of 363 VBM studies of the same psychiatric disorders with 14,027 patients and 14,504 normal controls were included (Table S2 and Fig. S3, S4). Peak coordinates with decreased and increased volumes for each study were separately extracted. VBM meta-analysis was also performed with the abovementioned MKDA algorithm. To reduce the effects of varying numbers of studies across

disorders, maps of decreased and increased gray matter were separately created by performing a meta-analysis of the studies in which an equal number of VBM studies (Decreased: 19, Increased: 3) was randomly (N = 100) extracted for each disorder and further pooled. Finally, we separately performed cross-voxel Pearson correlation analysis between the average of the hypo- and hyperconnectivity maps and gray matter values to examine the structural substrates of altered functional connectivity.

Correlation Analysis between Network Connectivity and Cognitive Performance (Datasets 1 and 3)

Next, we used the SB-FC meta-dataset and the HCP dataset to examine which aspects of cognitive function are associated with the neural networks that show altered functional connectivity across psychiatric disorders. This procedure involved the following 3 steps:

i) Using Dataset 1, we separately constructed binary networks of hypo- and hyperconnectivity based on the seed regions (SEED nodes) within the neurocognitive networks and the regions showing between-group differences (TARGET nodes) in the included studies (Fig. S5). Each seed coordinate from an individual study was smoothed with a 1-cm^3 sphere and compared with the high-resolution 1024-region template (36) (see Supplement). In each of the contrasts, an edge was defined as a pair of SEED and TARGET nodes. To assess whether a certain edge had a significantly greater frequency than expected by chance across the included contrasts, a nonparametric permutation test (N = 10,000) was performed with network-based statistic (NBS) correction (37) (Fig. S6 and Supplement). The result was a pattern of hypo- and hyperconnectivity that significantly appeared across psychiatric disorders. Next, we divided this hypo- and hyperconnectivity pattern into within- and between-network patterns for each of our three cognitive networks of interest, namely DMN, FPN and SN.

ii) To test whether this pattern of hypo- and hyperconnectivity was associated with cognitive

performance on behavioral tests, we used Dataset 3, derived from the R-fMRI and broad cognitive assessment data of 766 healthy participants. For each subject, based on a 1,024 high-resolution parcellation (36), a symmetric 1024 × 1024 functional connectivity matrix was constructed from the Pearson correlations between the time courses of each pair of regions. For each individual, we extracted the corresponding behavioral scores of 12 items involved in general cognitive function (see Supplement).

iii) For each of the 766 healthy subjects and for each group of edges, we computed the average correlation coefficients from the correlation matrix. Then, we calculated Spearman correlations between the average correlation coefficient of the edges and each of the 12 behavior scores across subjects (see Supplement); statistical inferences for each group of edges were made at $p < 0.05$ after Bonferroni correction (i.e., uncorrected $p < 0.05/6$, where 6 represents the number of groups among network connectivity).

Results

Altered Functional Connectivity within and between Neurocognitive Networks

The SB-FC meta-analysis revealed common alterations in functional connectivity within and between our three neurocognitive networks (the DMN, FPN and SN) (Fig. 1A; Table S3).

Within-Network alterations: Psychiatric disorders showed functional alterations between the DMN seeds and regions of the mPFC and PCC, between the FPN seeds and the dmPFC, and between the SN seeds and regions of the dACC and right insula (Fig. 1B; Table S4). These alterations were not moderated by age, gender, comorbidity, or medication status ($p > 0.05$).

Between-Network alterations: For the DMN, psychiatric disorders were characterized by functional alterations between the DMN seeds and the orbital frontal cortex in the FPN, as well as

regions of the dACC and left insula in the SN (Fig. 1B; Table S4). For the FPN, psychiatric disorders were associated with functional alterations between the FPN seeds and the rostromedial PFC (rmPFC) in the DMN as well as regions of the right insula and caudate in the SN (Fig. 1B; Table S4). For the SN, psychiatric disorders were characterized by functional alterations between the SN seeds and the dlPFC in the FPN, as well as regions of the rmPFC and left temporal pole (TP) within the DMN (Fig. 1B; Table S4). Moreover, additional meta-analyses of studies that had removed head movement and global signal did not change our main findings (Fig. S7 and S8). These alterations were not moderated by age, gender, comorbidity, or medication status ($p > 0.05$).

Hypo- versus Hyperconnectivity across Psychiatric Disorders

Network alterations were further characterized in terms of hypo- versus hyperconnectivity in patients relative to healthy controls (Table S5).

Within- and Between-Network Hypoconnectivity: Hypoconnectivity was observed within both the ventral DMN (e.g., the mPFC, vACC and PCC) and the SN (e.g., the dACC and left insula) (Fig. 2; Table S6). Moreover, hypoconnectivity was expressed between the DMN seeds and regions of the dACC and the ventral insula in the SN as well as between the FPN seeds and the putamen in the SN (Fig. 2A and 2B; Table S6). The SN seeds revealed hypoconnectivity with regions of the PCC and left TP in the DMN as well as with regions of the dlPFC and temporoparietal junction (TPJ) in the FPN (Fig. 2C; Table S6). Thus, the SN showed hypoconnectivity with the DMN as well as the FPN.

Within- and Between-Network Hyperconnectivity: Hyperconnectivity was observed within both the dorsal DMN (e.g., the rmPFC and precuneus) and the FPN (e.g., the dmPFC) (Fig. 2; Table S6). Moreover, the DMN seeds showed hyperconnectivity with the dlPFC in the FPN and with the dorsal insula in the SN (Fig. 2A; Table S6). Hyperconnectivity was also expressed between the FPN seeds and the mPFC (BA9) in the DMN (Fig. 2B; Table S6) and between the SN seeds and the precentral cortex in

the sensorimotor network (SMN) (Fig. 2C; Table S6). Thus, the DMN showed hyperconnectivity with the dorsal SN as well as with the FPN. Taken together, these findings indicate that hypo- or hyperconnectivity is most evident in regions implicated in executive control, self-monitoring and salience orienting (17, 19, 20). Fig. 3 presents a summary of the disrupted neurocognitive networks architecture across psychiatric disorders. These functional alterations were not moderated by age, gender, comorbidity, or medication status ($p > 0.05$).

Common Gray Matter Reductions across Psychiatric Disorders

To investigate whether a potential common anatomical signature underlies the altered network connectivity, we performed a VBM meta-analysis of 363 studies using Dataset 2. This analysis revealed decreased gray matter volume in the mPFC, dACC, bilateral insula, dlPFC and TPJ, all of which are among the regions showing altered network-level functional connectivity (Fig. 4A; Table S7). No significant region with increased volume was found across psychiatric disorders. The structural loss was not moderated by age, gender, comorbidity, or medication status ($p > 0.05$). Moreover, we found significant positive correlations between both the regions showing functional hypo- and hyperconnectivity and the gray matter values ($ps < 1.0 \times 10^{-10}$, Fig. 4A). These findings indicate cross-modality disruptions within the neurocognitive networks.

Behavioral Correlates of Network Connectivity

Finally, we examined which aspects of cognitive function are associated with the neural networks that show altered functional connectivity across psychiatric disorders. To test this hypothesis, we separately identified hypo- and hyperconnectivity that significantly appeared across psychiatric disorders (Fig. S9, Table S8). Among those connections showing lower values in patients relative to healthy controls: within-network DMN-ventral DMN connectivity was positively associated with performance in spatial orientation ($r = 0.10$, $p = 0.006$) and inhibition control ($r = 0.11$, $p = 0.002$); between-network FPN-SN

connectivity was positively correlated with fluid intelligence ($r = 0.10$, $p = 0.008$) (Fig. 4B). Among those connections showing higher values in patients relative to healthy controls: between-network DMN-FPN connectivity was negatively correlated with behavioral performance in spatial orientation ($r = -0.12$, $p < 0.001$); within-network FPN-FPN connectivity was negatively associated with alertness ($r = -0.14$, $p < 0.001$) (Fig. 4B).

Discussion

Our study revealed three main findings: first, psychiatric disorders are associated with common alterations of functional connectivity within and between neurocognitive networks; second, common gray matter reductions within these neurocognitive networks are tightly associated with functional alterations; third, common network alterations appears to be localized in regions that subserve different aspects of cognitive performance. To our knowledge, this study is the first to provide meta-analytic evidence of shared connectivity alterations within and between networks associated with cognitive function. These findings suggest a shared mechanism of network interactions that contribute to the generalized cognitive deficits observed in psychiatric disorders.

Common Connectivity Alterations within and between Neurocognitive Networks

Consistent with our first hypothesis, our findings revealed disrupted functional connectivity within and between neurocognitive networks. There are at least two explanations. One possible explanation is that such reduced functional connectivity is the results of heightened genetic susceptibility to psychiatric disorders (15, 38). Consistent with this explanation, several studies have reported transdiagnostic genetic influences on major psychiatric disorders (39-42). A second possible explanation is that disrupted functional connectivity within and between neurocognitive networks is a marker of illness onset and/or progression, consistent with the observation that cognitive function deteriorates around the time an

individual develops a mental illness (16, 43).

During both the resting state and certain cognitive tasks, the SN plays a crucial role in modulating shifts between internal attention (which is largely subserved by the DMN) and external executive functions (which are largely subserved by the FPN) (16, 44-47). This coordination between executive function and internal and external attention is thought to be critically impaired in most psychiatric disorders (16, 20). Our findings extend the current literature by revealing that the SN exhibits hypoconnectivity with the FPN, which is involved in the processing of executive control and goal-directed regulation, and the DMN, which contributes to self-referential processing. In contrast, hyperconnectivity is evident between the dorsal SN and the DMN, as well as between the FPN and DMN (Fig. 3). This combination of hypo- and hyperconnectivity between the DMN and the SN is consistent with previous studies showing that distinct parts of the insula exhibit distinct patterns of functional connectivity in healthy subjects (48-50). The dorsal insula (characterized by hyperconnectivity with the DMN) is part of the cingulo-opercular subnetwork, which is critical for cognitive flexibility (51). In contrast, the ventral insula-dACC subnetwork (characterized by hypoconnectivity with the DMN) is part of the SN, which is thought to play a key role in motivational engagement (52). Thus, DMN coupling with different parts of the insula could reflect differential psychopathological presentations. We also found that the SN seeds were hyperconnected with the SMN, which plays a key role in the perception of external stimuli. A previous co-activation meta-analysis reported that the posterior insula, a component of the SN, is associated with sensorimotor processes (49), which suggests that basic sensory features of the environment have excessive influence on cognitive processing in the diseased brain (48). Thus, imbalanced communication between the SN and the SMN may help explain sensory processing alterations within a wider psychopathological profile in major psychiatric disorders (53-55).

Relationship between Functional Connectivity and Structural Perturbations

Consistent with our second hypothesis, our VBM meta-analysis revealed that common gray matter reductions were localized within the neurocognitive networks and tightly associated with functional alterations. This provides support to the notion that neurocognitive networks are susceptible to gray matter loss across multiple psychiatric disorders; in contrast, we detected no common gray matter reductions in regions that were part of other networks (e.g., sensory and visual). Converging neuroimaging evidence suggests that the pattern of connectivity dysfunction among neurocognitive networks corresponds to structural perturbations across psychiatric disorders (8), which suggests that the structural properties of the brain place constraints on functional interactions occurring within and between networks. Notably, the previous structural MRI study found the decreased volume in the regions of mPFC, dACC and insula, and increased volume in the striatum in the psychiatric disorders (8). The pattern of decreased gray matter volumes was similar with our findings, but we did not observe any commonly increased volume across psychiatric disorders. This discrepancy might be caused by several factors, such as differences in included disorders, meta-analytic algorithms and statistical methods and the inclusion of more up-to-date studies in the present meta-analysis. By combining R-fMRI and structural MRI data, our study extended the previous findings based on single-modality investigations.

Relationship between Functional Connectivity and Cognitive Performance

Consistent with our third hypothesis, functional connectivity within the DMN was correlated with performance on tasks involving distinct aspects of cognition, including spatial orientation and inhibition control. Owing to the reciprocal relationship between the “task-negative network” (DMN) and “task-positive network” (FPN and SN), studies have shown that suppression of the DMN is related to improved cognitive control in healthy individuals (56, 57). Hence, the present patterns of within-DMN alterations may reflect abnormal communication in internal self-monitoring processing and external

cognitive flexibility in psychiatric disorders (16, 35, 58, 59). Next, we observed that the DMN-FPN connectivity is associated with orientation. Previous studies have reported that connectivity between the DMN and FPN is important for the interplay between attention orientation and default mode processing, and that mood disorders are associated with disrupted switching between resting and task-context processing (13, 60). These studies support our finding that DMN-FPN connectivity is involved in orientation. In contrast, we found that fluid intelligence was associated with FPN-SN connectivity. This observation recapitulates the results of previous studies in which reduced connectivity between the dlPFC and insula was found during cognitive processing in major depression disorder (58, 61).

Limitations and Future Work

Several issues need to be further addressed. First, due to the limited number of studies on specific disorders, we were unable to examine diagnosis-specific network alteration. Even though when analyzed separately depressive disorder and schizophrenia appear to show distinct connectivity patterns (Fig. S10), additional studies will be required to draw robust conclusions about individual disorders. Second, in our current paper, differential weights of individual disorders in the number of included studies and sample size might have a disproportionate influence on the meta-analytic results. Future work with normalizing weights in each disorder might account for the overrepresentation of some disorders on the meta-analytic results. Third, given that only 30 studies reported mean head motion, we were unable to perform meta-regression analysis to remove the effects of head motion on our meta-analytic findings (62). In the future, the availability of more studies will allow the formal evaluation of the effects of head motion on connectivity patterns across psychiatric disorders. Fourth, in the seed-based connectivity studies, the boundaries of the functional networks are dependent on the choice of seed regions. Thus, in our study, anatomical heterogeneity in the seed regions may have an impact on the anatomical boundaries of canonical functional networks and the associated delineation of the connectivity patterns

across psychiatric disorders. Future studies should therefore test the anatomical effects of seed regions on the meta-analytic results. Fifth, although the present study detected differences in functional connectivity between patients with various psychiatric disorders and healthy controls, it is unclear whether these differences reflected deviation from the “normal range” of functional connectivity; this question would require a larger sample size to estimate normal individual variability across different ages and genders (63-65). Sixth, the orbitofrontal cortex and temporal lobes showed disrupted connectivity with the neurocognitive networks. Although functional image distortions were sensitive in these regions (66, 67), the observed gray matter changes in the VBM meta-analysis suggested structural substrates underlying the functional alterations across psychiatric disorders. Finally, we found statistically significant associations between brain connectivity and behavior. However, these associations were relatively modest, and as such can only explain a fraction of the inter-individual variance in network connectivity; other possible explanations for such variance might include individual differences in cognition and behavior that were not modelled in our meta-analysis.

Acknowledgments and disclosures

This work was supported by the Natural Science Foundation of China (Grant Nos. 81620108016, 91432115), Changjiang Scholar Professorship Award (Grant No., T2015027), Beijing Municipal Science & Technology Commission (Grant No. Z151100003915082 and Z161100004916027) and Fundamental Research Funds for the Central Universities (No 2017XTCX04 and 2015KJJCA13).

The authors report no biomedical financial interests or potential conflicts of interest.

References

1. Merikangas KR, He JP, Burstein M, Swanson SA, Avenevoli S, Cui L, et al. (2010): Lifetime prevalence of mental disorders in U.S. adolescents: results from the National Comorbidity Survey Replication--Adolescent Supplement (NCS-A). *J Am Acad Child Adolesc Psychiatry*. 49:980-989.

2. Insel T, Cuthbert B, Garvey M, Heinssen R, Pine DS, Quinn K, et al. (2010): Research domain criteria (RDoC): toward a new classification framework for research on mental disorders. *Am J Psychiatry*. 167:748-751.

3. Sanislow CA, Pine DS, Quinn KJ, Kozak MJ, Garvey MA, Heinssen RK, et al. (2010): Developing constructs for psychopathology research: research domain criteria. *J Abnorm Psychol*. 119:631-639.

4. Zald DH, Lahey BB (2017): Implications of the hierarchical structure of psychopathology for psychiatric neuroimaging. *Biological Psychiatry: Cognitive Neuroscience and Neuroimaging*.

5. Caspi A, Houts RM, Belsky DW, Goldman-Mellor SJ, Harrington H, Israel S, et al. (2014): The p Factor: One General Psychopathology Factor in the Structure of Psychiatric Disorders? *Clin Psychol Sci*. 2:119-137.

6. Kim H, Eaton NR (2015): The hierarchical structure of common mental disorders: Connecting multiple levels of comorbidity, bifactor models, and predictive validity. *J Abnorm Psychol*. 124:1064-1078.

7. Shanmugan S, Wolf DH, Calkins ME, Moore TM, Ruparel K, Hopson RD, et al. (2016): Common and Dissociable Mechanisms of Executive System Dysfunction Across Psychiatric Disorders in Youth. *Am J Psychiatry*. 173:517-526.

8. Goodkind M, Eickhoff SB, Oathes DJ, Jiang Y, Chang A, Jones-Hagata LB, et al. (2015): Identification of a common neurobiological substrate for mental illness. *JAMA Psychiatry*. 72:305-315.

9. Millan MJ, Agid Y, Brune M, Bullmore ET, Carter CS, Clayton NS, et al. (2012): Cognitive

dysfunction in psychiatric disorders: characteristics, causes and the quest for improved therapy. *Nat Rev Drug Discov*. 11:141-168.

10. Elliott ML, Romer A, Knodt AR, Hariri AR (2018): A Connectome-wide Functional Signature of Transdiagnostic Risk for Mental Illness. *Biol Psychiatry*.

11. Sharma A, Wolf DH, Ciric R, Kable JW, Moore TM, Vandekar SN, et al. (2017): Common Dimensional Reward Deficits Across Mood and Psychotic Disorders: A Connectome-Wide Association Study. *Am J Psychiatry*. 174:657-666.

12. Xia CH, Ma Z, Ciric R, Gu S, Betzel RF, Kaczkurkin AN, et al. (2018): Linked dimensions of psychopathology and connectivity in functional brain networks. *Nat Commun*. 9:3003.

13. Williams LM (2016): Precision psychiatry: a neural circuit taxonomy for depression and anxiety. *Lancet Psychiatry*. 3:472-480.

14. Rubinov M, Bullmore E (2013): Fledgling pathoconnectomics of psychiatric disorders. *Trends Cogn Sci*. 17:641-647.

15. Buckholtz JW, Meyer-Lindenberg A (2012): Psychopathology and the human connectome: toward a transdiagnostic model of risk for mental illness. *Neuron*. 74:990-1004.

16. Menon V (2011): Large-scale brain networks and psychopathology: a unifying triple network model. *Trends Cogn Sci*. 15:483-506.

17. Anticevic A, Cole MW, Murray JD, Corlett PR, Wang XJ, Krystal JH (2012): The role of default network deactivation in cognition and disease. *Trends Cogn Sci*. 16:584-592.

18. Wager TD, Smith EE (2003): Neuroimaging studies of working memory: a meta-analysis. *Cogn Affect Behav Neurosci*. 3:255-274.

19. Cole MW, Reynolds JR, Power JD, Repovs G, Anticevic A, Braver TS (2013): Multi-task connectivity reveals flexible hubs for adaptive task control. *Nat Neurosci*. 16:1348-1355.

20. Uddin LQ (2015): Salience processing and insular cortical function and dysfunction. *Nat Rev Neurosci*. 16:55-61.

21. Zhang J, Wang J, Wu Q, Kuang W, Huang X, He Y, et al. (2011): Disrupted brain connectivity networks in drug-naive, first-episode major depressive disorder. *Biol Psychiatry*. 70:334-342.

22. Gong Q, Hu X, Pettersson-Yeo W, Xu X, Lui S, Crossley N, et al. (2017): Network-Level Dysconnectivity in Drug-Naive First-Episode Psychosis: Dissociating Transdiagnostic and Diagnosis-Specific Alterations. *Neuropsychopharmacology*. 42:933-940.

23. Xia M, He Y (2017): Functional connectomics from a "big data" perspective. *Neuroimage.*

24. Crossley NA, Mechelli A, Scott J, Carletti F, Fox PT, McGuire P, et al. (2014): The hubs of the human connectome are generally implicated in the anatomy of brain disorders. *Brain*. 137:2382-2395.

25. Sha Z, Xia M, Lin Q, Cao M, Tang Y, Xu K, et al. (2017): Meta-Connectomic Analysis Reveals Commonly Disrupted Functional Architectures in Network Modules and Connectors across Brain Disorders. *Cerebral Cortex*.1-16.

26. Wager TD, Lindquist MA, Nichols TE, Kober H, Van Snellenberg JX (2009): Evaluating the consistency and specificity of neuroimaging data using meta-analysis. *Neuroimage*. 45:S210-221.

27. Kaiser RH, Andrews-Hanna JR, Wager TD, Pizzagalli DA (2015): Large-Scale Network Dysfunction in Major Depressive Disorder: A Meta-analysis of Resting-State Functional Connectivity. *JAMA Psychiatry*. 72:603-611.

28. Wager TD, Jonides J, Reading S (2004): Neuroimaging studies of shifting attention: a meta-analysis. *Neuroimage*. 22:1679-1693.

29. Nee DE, Wager TD, Jonides J (2007): Interference resolution: insights from a meta-analysis of neuroimaging tasks. *Cogn Affect Behav Neurosci*. 7:1-17.

30. Power JD, Barnes KA, Snyder AZ, Schlaggar BL, Petersen SE (2012): Spurious but systematic

correlations in functional connectivity MRI networks arise from subject motion. *Neuroimage*. 59:2142-2154.

31. Van Dijk KR, Sabuncu MR, Buckner RL (2012): The influence of head motion on intrinsic functional connectivity MRI. *Neuroimage*. 59:431-438.

32. Murphy K, Fox MD (2017): Towards a consensus regarding global signal regression for resting state functional connectivity MRI. *Neuroimage*. 154:169-173.

33. Fox MD, Zhang D, Snyder AZ, Raichle ME (2009): The global signal and observed anticorrelated resting state brain networks. *J Neurophysiol*. 101:3270-3283.

34. Etkin A, Wager TD (2007): Functional neuroimaging of anxiety: a meta-analysis of emotional processing in PTSD, social anxiety disorder, and specific phobia. *Am J Psychiatry*. 164:1476-1488.

35. Dong D, Wang Y, Chang X, Luo C, Yao D (2017): Dysfunction of Large-Scale Brain Networks in Schizophrenia: A Meta-analysis of Resting-State Functional Connectivity. *Schizophr Bull*.

36. Zalesky A, Fornito A, Harding IH, Cocchi L, Yucel M, Pantelis C, et al. (2010): Whole-brain anatomical networks: does the choice of nodes matter? *Neuroimage*. 50:970-983.

37. Zalesky A, Fornito A, Bullmore ET (2010): Network-based statistic: identifying differences in brain networks. *Neuroimage*. 53:1197-1207.

38. Fornito A, Bullmore ET (2012): Connectomic intermediate phenotypes for psychiatric disorders. *Front Psychiatry*. 3:32.

39. Gandal MJ, Haney JR, Parikshak NN, Leppa V, Ramaswami G, Hartl C, et al. (2018): Shared molecular neuropathology across major psychiatric disorders parallels polygenic overlap. *Science*. 359:693-697.

40. Cross-Disorder Group of the Psychiatric Genomics C, Lee SH, Ripke S, Neale BM, Faraone SV, Purcell SM, et al. (2013): Genetic relationship between five psychiatric disorders estimated from

genome-wide SNPs. *Nat Genet*. 45:984-994.

41. Smoller JW, Andreassen OA, Edenberg HJ, Faraone SV, Glatt SJ, Kendler KS (2018): Psychiatric genetics and the structure of psychopathology. *Mol Psychiatry*.

42. Brainstorm C, Anttila V, Bulik-Sullivan B, Finucane HK, Walters RK, Bras J, et al. (2018): Analysis of shared heritability in common disorders of the brain. *Science*. 360.

43. Peters SK, Dunlop K, Downar J (2016): Cortico-Striatal-Thalamic Loop Circuits of the Salience Network: A Central Pathway in Psychiatric Disease and Treatment. *Front Syst Neurosci*. 10:104.

44. Seeley WW, Menon V, Schatzberg AF, Keller J, Glover GH, Kenna H, et al. (2007): Dissociable intrinsic connectivity networks for salience processing and executive control. *J Neurosci*. 27:2349-2356.

45. Dosenbach NU, Fair DA, Miezin FM, Cohen AL, Wenger KK, Dosenbach RA, et al. (2007): Distinct brain networks for adaptive and stable task control in humans. *Proc Natl Acad Sci U S A*. 104:11073-11078.

46. Chen AC, Oathes DJ, Chang C, Bradley T, Zhou ZW, Williams LM, et al. (2013): Causal interactions between fronto-parietal central executive and default-mode networks in humans. *Proc Natl Acad Sci U S A*. 110:19944-19949.

47. McTeague LM, Huemer J, Carreon DM, Jiang Y, Eickhoff SB, Etkin A (2017): Identification of Common Neural Circuit Disruptions in Cognitive Control Across Psychiatric Disorders. *Am J Psychiatry*. 174:676-685.

48. Chang LJ, Yarkoni T, Khaw MW, Sanfey AG (2013): Decoding the role of the insula in human cognition: functional parcellation and large-scale reverse inference. *Cereb Cortex*. 23:739-749.

49. Deen B, Pitskel NB, Pelphrey KA (2011): Three systems of insular functional connectivity identified with cluster analysis. *Cereb Cortex*. 21:1498-1506.

50. Power JD, Cohen AL, Nelson SM, Wig GS, Barnes KA, Church JA, et al. (2011): Functional

network organization of the human brain. *Neuron*. 72:665-678.

51. Touroutoglou A, Hollenbeck M, Dickerson BC, Feldman Barrett L (2012): Dissociable large-scale networks anchored in the right anterior insula subserve affective experience and attention. *Neuroimage*. 60:1947-1958.

52. Nelson SM, Dosenbach NU, Cohen AL, Wheeler ME, Schlaggar BL, Petersen SE (2010): Role of the anterior insula in task-level control and focal attention. *Brain Struct Funct*. 214:669-680.

53. Van Rheenen TE, Rossell SL (2013): Auditory-prosodic processing in bipolar disorder; from sensory perception to emotion. *J Affect Disord*. 151:1102-1107.

54. McGhie A, Chapman J (1961): Disorders of attention and perception in early schizophrenia. *Br J Med Psychol*. 34:103-116.

55. Piek JP, Dyck MJ (2004): Sensory-motor deficits in children with developmental coordination disorder, attention deficit hyperactivity disorder and autistic disorder. *Hum Mov Sci*. 23:475-488.

56. Hampson M, Driesen N, Roth JK, Gore JC, Constable RT (2010): Functional connectivity between task-positive and task-negative brain areas and its relation to working memory performance. *Magn Reson Imaging*. 28:1051-1057.

57. Kelly AM, Uddin LQ, Biswal BB, Castellanos FX, Milham MP (2008): Competition between functional brain networks mediates behavioral variability. *Neuroimage*. 39:527-537.

58. Gong Q, He Y (2015): Depression, neuroimaging and connectomics: a selective overview. *Biol Psychiatry*. 77:223-235.

59. Sheffield JM, Barch DM (2016): Cognition and resting-state functional connectivity in schizophrenia. *Neurosci Biobehav Rev*. 61:108-120.

60. Fornito A, Harrison BJ, Zalesky A, Simons JS (2012): Competitive and cooperative dynamics of large-scale brain functional networks supporting recollection. *Proc Natl Acad Sci U S A*.

109:12788-12793.

61. Lui S, Wu Q, Qiu L, Yang X, Kuang W, Chan RC, et al. (2011): Resting-state functional connectivity in treatment-resistant depression. *Am J Psychiatry*. 168:642-648.

62. Eickhoff SB, Nichols TE, Laird AR, Hoffstaedter F, Amunts K, Fox PT, et al. (2016): Behavior, sensitivity, and power of activation likelihood estimation characterized by massive empirical simulation. *Neuroimage*. 137:70-85.

63. Marquand AF, Rezek I, Buitelaar J, Beckmann CF (2016): Understanding Heterogeneity in Clinical Cohorts Using Normative Models: Beyond Case-Control Studies. *Biol Psychiatry*. 80:552-561.

64. Wolfers T, Doan NT, Kaufmann T, Alnaes D, Moberget T, Agartz I, et al. (2018): Mapping the Heterogeneous Phenotype of Schizophrenia and Bipolar Disorder Using Normative Models. *JAMA Psychiatry*.

65. Pinaya WH, Mechelli A, Sato JR (2018): Using deep autoencoders to identify abnormal brain structural patterns in neuropsychiatric disorders: A large‐scale multi‐sample study. *Human brain mapping*.

66. Ojemann JG, Akbudak E, Snyder AZ, McKinstry RC, Raichle ME, Conturo TE (1997): Anatomic localization and quantitative analysis of gradient refocused echo-planar fMRI susceptibility artifacts. *Neuroimage*. 6:156-167.

67. Lipschutz B, Friston KJ, Ashburner J, Turner R, Price CJ (2001): Assessing study-specific regional variations in fMRI signal. *Neuroimage*. 13:392-398.

68. Xia M, Wang J, He Y (2013): BrainNet Viewer: a network visualization tool for human brain connectomics. *PLoS One*. 8:e68910.

Table 1. Datasets and Demographics Included in This Study.

	Dataset 1		Dataset 2		Dataset 3
	Patients	Controls	Patients	Controls	Healthy
Subjects (N)	8,298	8,165	14,027	14,504	766
Gender (N,male/female)	4809/3247[a]	4594/3328[a]	8083/5693[a]	8085/6172[a]	331/435
Age (years, mean ± std)	28.89 ± 11.79[b]	28.63 ± 11.35[b]	31.87 ± 12.42[b]	31.12 ± 12.08[b]	22 - 36+

[a] Gender information was extracted from available 237 and 352 studies by summing up the exact numbers in each study of Datasets 1 and 2, respectively.

[b] Age information was extracted by averaging the mean and standard deviation values across 235 and 355 studies in Datasets 1 and 2, respectively.

Figure Legends

Figure 1. Functional Connectivity Differences between Psychiatric Disorders and Healthy Controls.

A. Spatial distribution of our three neurocognitive networks of interest. B. Regions showing functional alterations with seeds in the DMN, FPN and SN respectively, with pooling across patients with hypo- and hyperconnectivity. The three neurocognitive networks were mapped on the cortical surface using BrainNet Viewer(68). Abbreviations: DMN, default-mode network; FPN, frontoparietal network; SN, salience network; Cau, caudate; dACC, dorsal anterior cingulate cortex; dlPFC, dorsolateral prefrontal cortex; dmPFC, dorsomedial prefrontal cortex; Ins, insula; mPFC, medial prefrontal cortex; OFC, orbital frontal cortex; PCC, posterior cingulate cortex; TP, temporal pole; *eb*, extent-based threshold; *hb*, height-based threshold.

Figure 2. Hypo- and Hyperconnectivity across Psychiatric Disorders.

A. Regions showing trans-diagnostic DMN hypo- and hyperconnectivity. B. Regions showing trans-diagnostic FPN hypo- and hyperconnectivity. C. Regions showing trans-diagnostic SN hypo- and hyperconnectivity. Abbreviations: DMN, default-mode network; FPN, frontoparietal network; SN, salience network; Cau, caudate; dACC, dorsal anterior cingulate cortex; dlPFC, dorsolateral prefrontal cortex; dmPFC, dorsomedial prefrontal cortex; Ins, insula; mPFC, medial prefrontal cortex; OFC, orbital frontal cortex; PCC, posterior cingulate cortex; Put, putamen; SFG, superior frontal gyrus; PSC, precentral cortex; TP, temporal pole; TPJ, temporo-parietal junction; *eb*, extent-based threshold; *hb*, height-based threshold.

Figure 3. Disrupted Functional Architecture of Neurocognitive Networks across Psychiatric Disorders.

Visual representation of the disrupted functional architecture of neurocognitive networks across psychiatric disorders identified in our investigation. The DMN seeds were hypoconnected with the ventral DMN (represented as "V" in the left panel), and hyperconnected with the dorsal DMN (represented as "D" in the right panel). In addition, the SN exhibited hypoconnectivity with the FPN and DMN. In contrast, hyperconnectivity was evident between the SN and DMN, between the FPN and DMN, as well as between the SN and SMN. The blue and red arrows separately indicate hypo- and hyperconnectivity; and the circular arrows indicate within-network connectivity alterations. Abbreviations: DMN, default-mode network; FPN, frontoparietal network; SN, salience network.

Figure 4. Structural Substrates of Functional Connectivity Alterations and Its Association with Cognitive Performance.

A. Decreased gray matter volume in patients relative to controls (left panel). Positive correlation between the regions showing functional alterations and structural perturbations (right panel). B. Relationship between functional connections showing decreases and increases in patients and behavioral cognitive test performance in healthy volunteers. Here the left panel shows a spring-embedded layout of nodes and edges that significantly decreased (i.e. hypoconnectivity) and increased (i.e. hyperconnectivity) within and between the DMN, FPN and SN networks across psychiatric disorders. The right panel shows the relationship between the network-connectivity and cognitive performance. Abbreviations: vDMN, ventral default-mode network; dDMN, dorsal default-mode network; FPN, frontoparietal network; SMN, sensory-motor network; SN, salience network; *eb*, extent-based threshold; *hb*, height-based threshold.

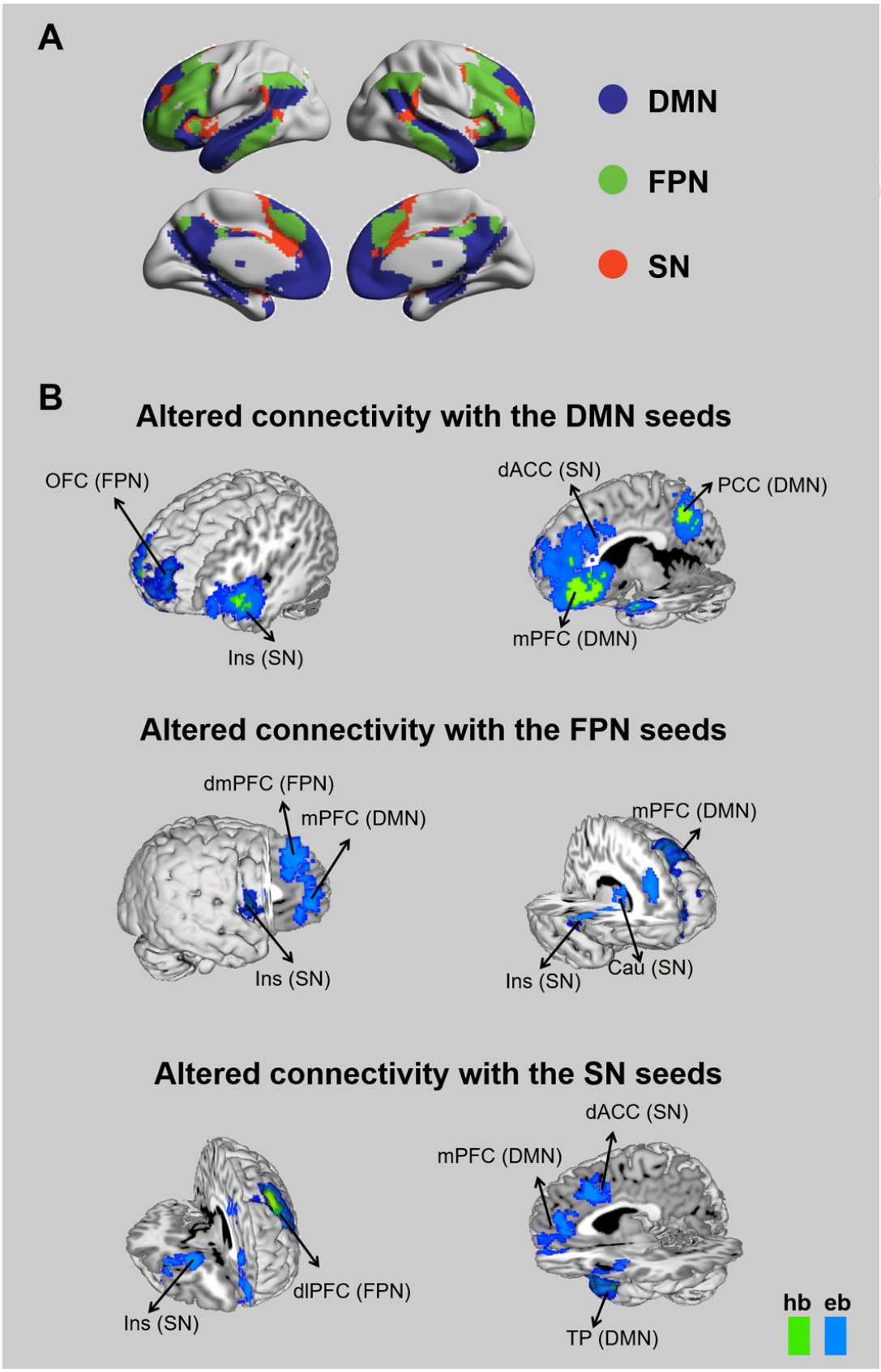
A
DMN
FPN
SN
B
Altered connectivity with the DMN seeds
OFC (FPN)
Ins (SN)
dACC (SN)
PCC (DMN)
mPFC (DMN)
Altered connectivity with the FPN seeds
dmPFC (FPN)
mPFC (DMN)
Ins (SN)
mPFC (DMN)
Ins (SN)
Cau (SN)
Altered connectivity with the SN seeds
dlPFC (FPN)
Ins (SN)
dACC (SN)
mPFC (DMN)
TP (DMN)
hb
eb

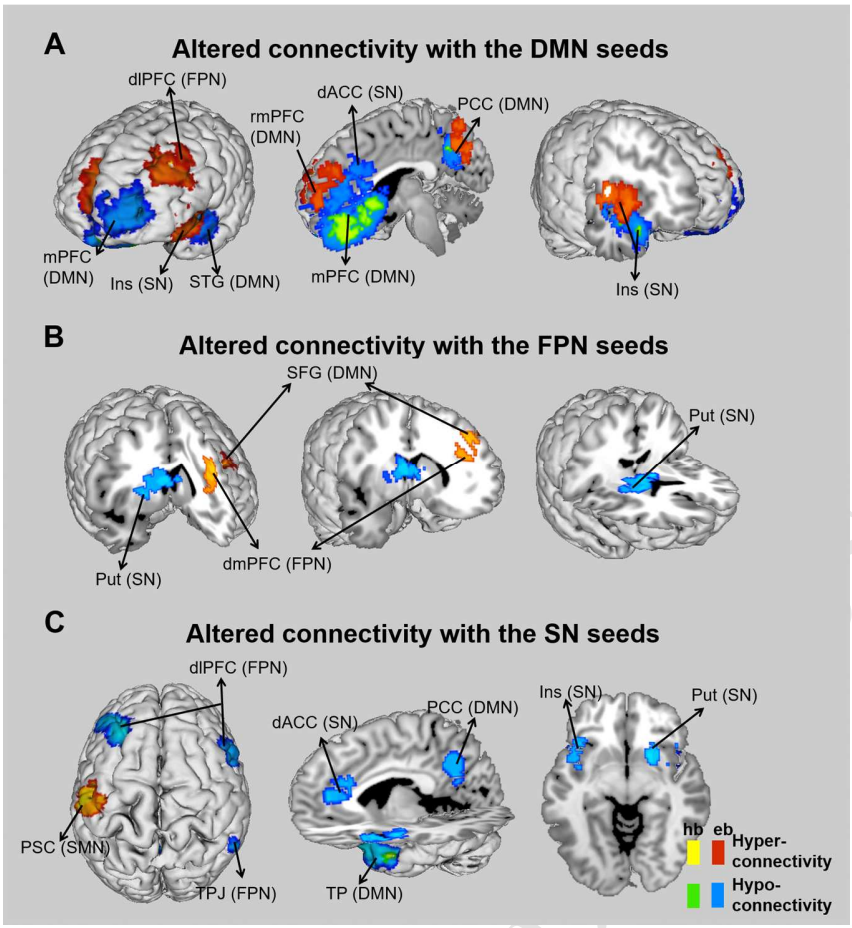

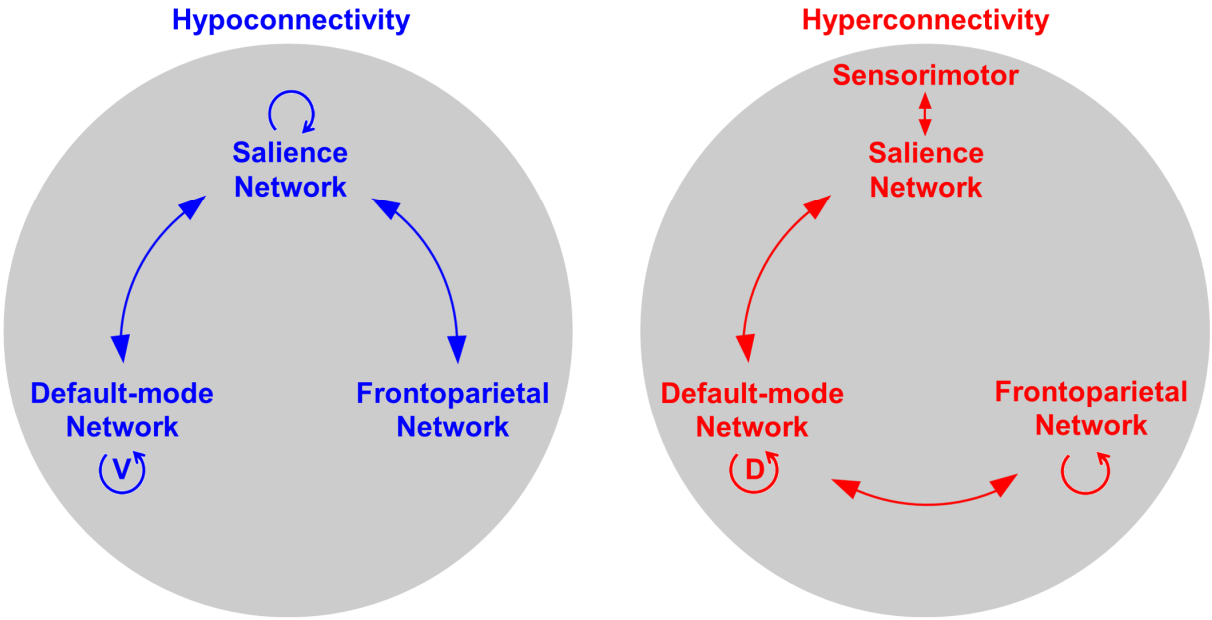

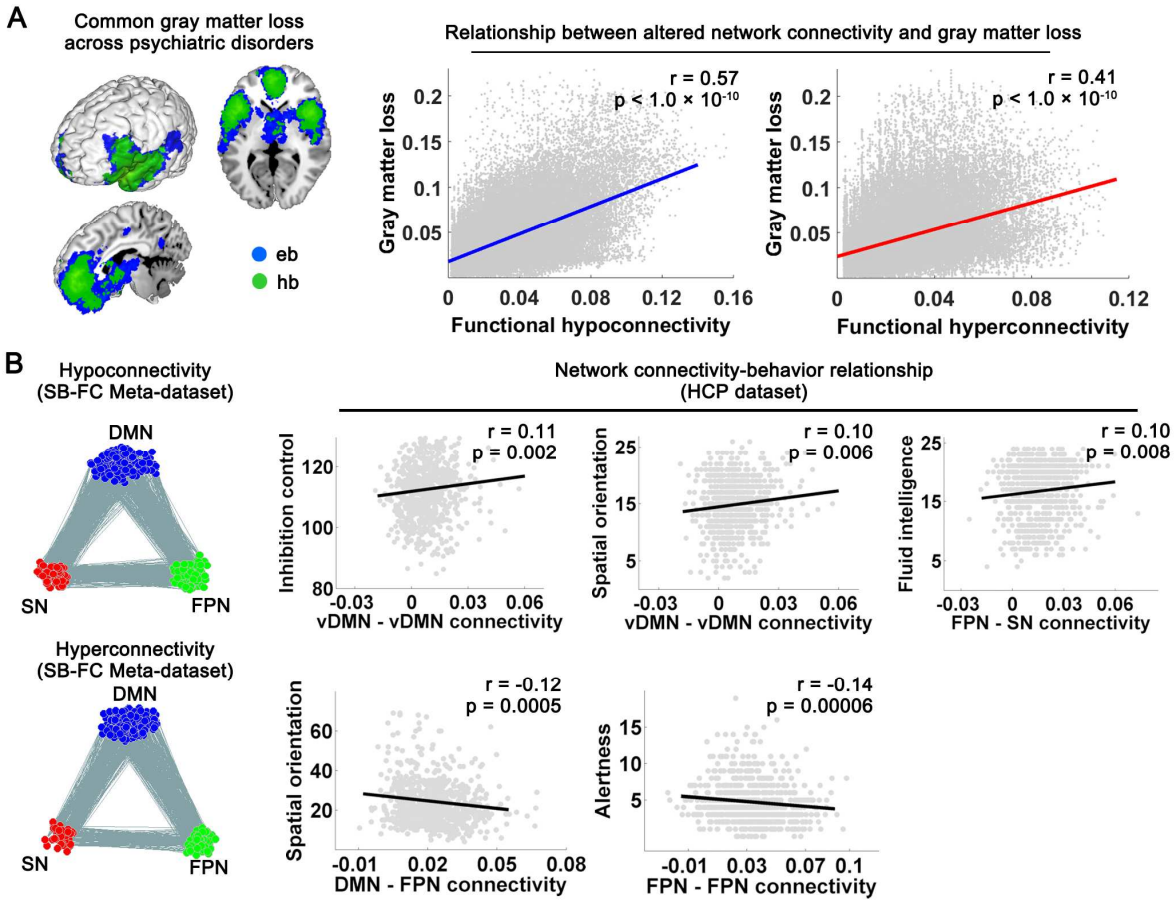
A
Common gray matter loss
across psychiatric disorders
eb
hb
Relationship between altered network connectivity and gray matter loss
r = 0.57
p < 1.0 × 10-10
Gray matter loss
Functional hypoconnectivity
r = 0.41
p < 1.0 × 10-10
Gray matter loss
Functional hyperconnectivity
B
Hypoconnectivity
(SB-FC Meta-dataset)
DMN
SN
FPN
Network connectivity-behavior relationship
(HCP dataset)
r = 0.11
p = 0.002
Inhibition control
vDMN - vDMN connectivity
r = 0.10
p = 0.006
Spatial orientation
vDMN - vDMN connectivity
r = 0.10
p = 0.008
Fluid intelligence
FPN - SN connectivity
Hyperconnectivity
(SB-FC Meta-dataset)
DMN
SN
FPN
r = -0.12
p = 0.0005
Spatial orientation
DMN - FPN connectivity
r = -0.14
p = 0.00006
Alertness
FPN - FPN connectivity

Common Dysfunction of Large-Scale Neurocognitive Networks Across Psychiatric Disorders

Supplementary Information

Supplementary Methods

Study Selection Criteria

Seed-Based Functional Connectivity (SB-FC) Meta-Analysis

The selected studies were restricted to original resting-state functional MRI (R-fMRI) studies using whole brain seed-based functional connectivity to compare patients with Axis I psychiatric diagnoses and controls. The keywords used in the searches were as follows: 1) imaging modalities: 'functional MRI', 'fMRI' or 'resting state'; 2) analysis strategies: 'connectivity'; and 3) disorders: 'attention deficit hyperactivity', 'ADHD', 'anorexia nervosa', 'anxiety disorder', 'autism', 'Asperger', 'ASD', 'conduct disorder', 'bipolar disorder', 'unipolar depress*', 'dissociative disorder', 'dysthymia', 'dyslexia', 'depress*', 'hallucination', 'insomnia', 'eating disorder', 'manic disorder', 'obsessive-compulsive', 'obsessive compulsive', 'OCD', 'panic disorder', 'posttraumatic stress', 'post-traumatic stress', 'post traumatic stress', 'PTSD', 'personality disorder', 'borderline personality', 'phobia' 'psychosis', 'psychotic', 'Rett syndrome', 'sleeping disorder', 'schizophreni*', 'somatization disorder', 'Tourette syndrome'. Every combination of these three categories of keywords was searched to identify relevant papers in each database.

The inclusion criteria were as follows:

1) Studies which reported the coordinates in standard stereotaxic spaces (i.e., the Talairach or Montreal Neurological Institute (MNI) spaces).

2) The results were reported using a statistical threshold of $p < 0.05$ (corrected) or $p < 0.001$ (uncorrected).

The exclusion criteria were as follows:

1) The studies did not include a healthy control group.

2) There were only high-risk or sibling groups.

3) The studies reported only the results of task-based fMRI.

4) SB-FC analysis was not performed in the whole brain.

5) The results of the whole-brain analysis did not reach statistical significance.

6) The studies only included seeds within the cerebellum.

7) The peak coordinates were not reported.

8) The articles were not written in English.

Several rules were subsequently applied to further refine the selection of studies or results as follows: 1) If between-group differences were reported at both the baseline and follow-up stages, only the differences at baseline were selected. 2) If the results were reported both with and without a gray matter correction, the corrected results were selected. 3) If the statistical analysis was repeated different parameters (e.g., with and without head motion correction; with and without removal of global signal), only the main results were selected. 4) Psychiatric disorders investigated in few studies were excluded (N < 5). Following the application of these criteria, 242 SB-FC studies of 8 psychiatric disorders with 8,298 patients and 8,165 normal controls were included. The 8 psychiatric disorders comprised attention deficit hyperactivity disorder (ADHD), anxiety disorders (ANX), autism spectrum disorder (ASD), bipolar affective disorder (BD), depressive disorder (DPD), obsessive-compulsive disorder (OCD), posttraumatic stress disorder (PTSD) and schizophrenia (SCZ) (Fig. S1 and Table S1).

Voxel-Based Morphometry (VBM) Meta-Analysis

A similar procedure was followed to select the studies related to VBM analysis. Notably, the keywords used in the searches were as follows: 1) imaging modalities: ‘MRI’ or ‘magnetic resonance image’; 2) analysis strategies: ‘voxel based morphometry’ or ‘VBM’; and 3) disorders: ‘attention deficit hyperactivity’, ‘ADHD’, ‘anorexia nervosa’, ‘anxiety disorder’, ‘autism’, ‘Asperger’, ‘ASD’, ‘conduct disorder’, ‘bipolar disorder’, ‘unipolar depress*’, ‘dissociative disorder’, ‘dysthymia’, ‘dyslexia’, ‘depress*’, ‘hallucination’, ‘insomnia’, ‘eating disorder’, ‘manic disorder’, ‘obsessive-compulsive’, ‘obsessive compulsive’, ‘OCD’, ‘panic disorder’, ‘posttraumatic stress’, ‘post-traumatic stress’, ‘post traumatic stress’, ’PTSD’, ‘personality disorder’, ‘borderline personality’, ‘phobia’ ‘psychosis’, ‘psychotic’, ‘Rett syndrome’, ‘sleeping disorder’, ‘schizophreni*’, ‘somatization disorder’, ‘Tourette syndrome’. Every combination of these three categories of keywords was searched

to identify relevant papers in each database. The inclusion and exclusion criteria were similar to those of the SB-FC meta-analysis described above. Following the application of these criteria, 363 VBM studies of the same 8 psychiatric disorders with 14,027 patients and 14,504 controls were included (Fig. S3 and Table S2).

Data Extraction

For the SB-FC meta-analysis, based on our previous modular detection in 143 healthy subjects (1), we first identified the neurocognitive network parcellations mentioned in Menon's study (2), including the default-mode network (DMN), the frontoparietal network (FPN) and the salience networks (SN). Then, seeds were separately categorized into triple seed networks. If the seed was a spherical region of interest (ROI) with a peak coordinate, it was directly categorized into our voxel-wise brain network on the basis of the location of the peak coordinate. If the seed was an anatomical region from the prior template or standard brain atlas, the ROI was aligned with the brain network mask, and the overlapping proportion between the ROI and each of the network templates was completely calculated. We determined the functional network in which the seed ROI was located by checking for an overlapping ratio above 40%.

Multilevel Kernel Density Analysis (MKDA)

In the MKDA analysis, we first extracted the peak coordinates to result in an indicator map (IM) for each study. Subsequently, a weighted average of all the IM maps was computed to assess the density of effects. We then performed Monte Carlo simulation (10,000 iterations) with the weighted average density maps to establish a familywise error (FWE) threshold for multiple comparisons. In the simulation, the locations of significant effects from IMs were randomized within a gray-matter mask 10,000 times, producing a null hypothesis distribution of the density of effects expected by chance. Density maps can be thresholded by two approaches: height-based (hb) and extent-based (eb) thresholding. For each stimulation in the former threshold, the maximum across-study density statistic (P) over the whole brain is saved. The critical Familywise Error Rate (FWER)-controlled threshold is the proportion that

exceeds the whole-brain maximum in 95% of the Monte Carlo maps — controlling for the chance of seeing false positives anywhere in the brain at $p < 0.05$ corrected. For each stimulation in the latter threshold, the largest cluster of contiguous voxels was saved, and a cluster extent threshold was set at the 99.999th percentile of these values across iterations — controlling for the chance of seeing false positives anywhere in the brain at $p < 0.001$ corrected.

Post Hoc Analyses

In order to assess whether the results were independent of the inclusion of a specific study, we performed a series of further meta-analyses with leave-one-study-out ("jackknife") validation. To accomplish this, the density statistic for each significant cluster was iteratively recomputed with each of the included studies separately omitted. Pearson correlation analysis was then performed between the original density map and each of the individual leave-one-out density maps. Fisher exact test was used to investigate moderation of effects by clinical and demographic factors, including comorbidity, medication status, age or gender. For these analyses, the proportion of studies within each clinical or demographic group reporting the effect was calculated, and differences in proportions were tested between groups.

Identification of Significantly Hypo- and Hyperconnectivity across Psychiatric Disorders (Dataset 1)

Construction of Hypo- and Hyperconnectivity Networks

We separately constructed binary networks of hypo- and hyperconnectivity based on the seed regions (SEED nodes) and the regions with between-groups differences (TARGET nodes). Regardless of hypo- and hyperconnectivity networks, we all extracted the SEEDs and TARGETs from the meta-analytic Dataset 1 and constructed separate SEED and TARGET binary networks. Each seed coordinate from an individual study was smoothed with 1 cm^3 sphere in a standard stereotactic space and compared with the high-resolution 1024-region template. The node was set to value of 1 if 20% or more of the SEED or TARGET nodes

overlapped with the regional volume defined by the 1024-region parcellation template. Thus, for each contrast, we obtained the binary SEED and TARGET matrices, in which an edge was defined as between the given SEED node and any of the TARGET nodes (Fig. S5).

Construction of a Null Model Based on Data Randomization

To assess whether a certain edge in a given experiment had a significantly greater frequency than expected by chance across the included contrasts, a nonparametric permutation test (N = 10,000) was performed with network-based statistic (NBS) correction (3). Specifically, for each edge, we counted the frequencies of the edges that appeared to be altered across contrasts. Then, for each permutation, we randomly allocated SEED and TARGET nodes in each of the included contrasts and computed the frequencies of the edge across all the contrasts in a random model. The process was iterated 10,000 times and formed a null distribution (Fig. S6). A primary threshold ($p < 0.0001$, uncorrected) was first applied to this null hypothesis for each link to define a set of suprathreshold links among which any connected components and their size (M, number of links) were then determined. To estimate the significance for each component, the null distribution of connected component size was empirically derived using a nonparametric permutation approach (1000 permutations). For each permutation, we randomly generated 1000 matrixes based on the above-mentioned approach. Combined with the matrix used to count the frequencies of edges across included studies, these matrixes were randomly reallocated into two groups and non-parameter tests were computed independently for each link. Then, the same primary threshold ($p < 0.0001$) was used to generate suprathreshold links among which the maximal connected component size was recorded. Finally, for a connected component of size M found in the correct grouping of matrixes generated by the included studies and null hypothesis, the corrected p-value was determined by finding the proportion of the 1000 permutations for which the maximal connected component was larger than M. Finally, we obtained a set of hypo- and hyperconnectivity that frequently appeared across psychiatric disorders.

R-fMRI Data and Cognitive Behavioral Tests of Healthy Subjects (Dataset 3)

Participants and Image Acquisition

This dataset was used to assess whether the network connectivity was associated with

cognitive function. The dataset was collected as part of the Washington University-Minnesota Consortium Human Connectome Project (4). The participants were recruited from Washington University (St. Louis, MO) and the surrounding area. All participants gave informed consent. The R-fMRI data used were from all parts of releases, consisting of data from 970 participants. R-fMRI data were collected over 2 days. On each day, 28 min of R-fMRI data across two runs were collected (56 min total), and the first run was only extracted for our study. A total of 97 and 13 subjects were excluded due to a lack of fMRI data runs and behavioral test scores, respectively. Furthermore, 27 subjects were excluded due to the identification of an arachnoid cyst, and 68 subjects were excluded due to larger head motion, with a criterion of 3 mm or 3°. Finally, the data of 766 subjects were included in the analyses. All the included subjects were healthy adults, ranging in age from 22 to > 36 years, and the gender ratio was 331/435 (male/female).

All subjects were scanned on a 3-T Siemens connectome-Skyra scanner (customized to achieve 100 mT m^{-1} gradient strength) with a 32-channel phased array head coil. This high spatial and temporal resolution was made possible through the use of multiband echo-planar imaging, with a simultaneous multi-slice acceleration factor of 8 (5). To aid in cross-subject registration and surface mapping, T1-weighted structural images with a resolution 0.7-mm isotropic were also acquired, and B0 field mapping was carried out to aid in correcting EPI distortions. The parameters were as follows: TR = 720 ms; TE = 33.1 ms; FA = 52°; bandwidth = 2,290 Hz/pixel, in-plane field of view = 208 × 180 mm, 72 slices, and 2.0 mm isotropic voxels. The resting-state data collection details for this data set can be found elsewhere (5, 6).

Image Preprocessing

In brief, the R-fMRI dataset preprocessing consisted of standard functional connectivity preprocessing strategies, including the removal of the first five volumes, slice timing correction, spatial volume correction, segment and normalization to an MNI space, which was performed using minimal preprocessing pipelines for the Human Connectome Project (4). Next, we removed the linear trend and nuisance time series (motion, ventricle, whole-brain, cerebrospinal fluid and white matter signals) using a linear regression. Finally, we performed temporal band pass filtering (0.01-0.1 Hz). Notably, 68 subjects were excluded for larger

head motion with a criterion of 3 mm or 3°.

Extraction of Cognitive Behavioral Scores

Apart from the R-fMRI data, for each subject from Dataset 3, we also extracted the corresponding behavioral scores of 12 items involved in the domain of general cognitive function, including episodic memory, executive function/cognitive flexibility, executive function/inhibition, fluid intelligence, language/reading decoding, language/vocabulary comprehension, processing speed, self-regulation/impulsivity, spatial orientation, sustained attention, verbal episodic memory and working memory.

Supplementary Results

First, to test whether the network dysfunction was affected by head movement, we replicated the SB-FC meta-analysis with 103 studies in which the results were obtained after regressing out head movement (7, 8). This analysis revealed altered functional connectivity within and between our three neurocognitive networks of interest, which was similar to the main findings (Fig. S7). We also compared the differences between the effect sizes of studies with and without regression of head motion and among the studies with 6, 12 and 24 head motion parameters. The results showed no statistically significant differences between the subsets of studies ($p > 0.05$), suggesting that head motion effects had little effect on our main results. Second, to test whether network dysfunction was affected by the global signal (GS) (9, 10), we separately performed the SB-FC meta-analysis of 129 studies with global signal regression (GSR) and 113 studies without GSR. The patterns of common alterations in functional connectivity within and between our three neurocognitive networks were replicated using studies both with and without GSR (Fig. S8). Moreover, the effect sizes of the studies did not differ for the two subsets of studies with and without GSR ($p > 0.05$), suggesting that global signal effects had little influence on our main results. Third, to assess whether the results were independent of each of the included studies, we performed further meta-analysis using the leave-one-out validation approach. We failed to find a disproportionate effect of any single study ($p < 0.001$); therefore, all of the initially included studies were retained in the analysis. Fourth, to evaluate whether the results for the DMN

network were biased by the fact that most of the studies focused on DPD and SCZ, we separately repeated the SB-FC meta-analysis of the DMN network after excluding studies on DPD and SCZ. This analysis yielded similar results to the previous meta-analysis of DMN dysfunction. In the meta-analysis of studies excluding DPD, functional alteration was observed within the DMN (e.g., the medial prefrontal cortex, ventral anterior cingulate cortex and posterior cingulate cortex) and between the DMN seeds and regions of the dorsal anterior cingulate cortex and ventral insula in the SN and regions of the dorsomedial and dorsolateral prefrontal cortex in the FPN (Fig. S10A). Similar patterns were also shown in the meta-analysis of studies excluding SCZ (Fig. S10B). To assess whether the meta-analytic results of altered DMN connectivity could be replicated in DPD and SCZ, we separately performed the meta-analysis of studies in both disorders, which revealed similar results to the previous meta-analysis of altered DMN connectivity. Specifically, DPD showed functional alteration within the DMN (e.g., posterior cingulate cortex) and between the DMN seeds and insula in the SN and dorsolateral prefrontal cortex in the FPN (Fig. S10C). Similarly, SCZ showed functional alteration within the DMN (e.g., ventromedial prefrontal cortex) and between the DMN seeds and dorsomedial prefrontal cortex in the FPN and the regions of insula and dorsal anterior cingulate cortex in the SN (Fig. S10D). Finally, to assess the robustness of the results, we repeated this analysis using a range of spherical kernel radii (from 10mm to 15mm), which recapitulated the results of our main meta-analysis (Fig. S11).

Table S1. Number of Studies, Patients and Controls Included in the SB-FC Meta-Analysis.

Disorders	Abbreviations	Studies	Patients	Controls
Attention deficit hyperactivity disorder	ADHD	16	374	395
Anxiety disorders	ANX	19	436	422
Autism spectrum disorder	ASD	29	1315	1371
Bipolar affective disorder	BD	18	493	524
Depressive disorder	DPD	63	2023	1839
Obsessive-compulsive disorder	OCD	16	481	459
Posttraumatic stress disorder	PTSD	15	492	450
Schizophrenia	SCZ	66	2684	2705
Total		242	8298	8165

Table S2. Number of Studies, Patients and Controls Included in the VBM Meta-Analysis.

Disorders	Abbreviations	Studies (Dec/Inc)	Patients	Controls
Attention deficit hyperactivity disorder	ADHD	24(24/5)	670	619
Anxiety disorders	ANX	19(19/5)	447	484
Autism spectrum disorder	ASD	28(28/12)	713	735
Bipolar affective disorder	BD	25(25/7)	836	1008
Depressive disorder	DPD	66(66/14)	2613	2958
Obsessive-compulsive disorder	OCD	27(27/10)	763	847
Posttraumatic stress disorder	PTSD	29(29/3)	494	599
Schizophrenia	SCZ	145(145/25)	7491	7254
Total		363(363/81)	14027	14504

Note: Dec and Inc respectively represent the number of included studies reporting decreased and increased volumes in the patients group compared with control group.

Table S3. Summary of Seed-Networks Included in SB-FC Meta-Analysis of Altered Connectivity.

Networks	ADHD	ANX	ASD	BD	DPD	OCD	PTSD	SCZ	Total studies
DMN	10	13	29	8	61	17	13	44	195
FPN	11	5	14	4	17	4	0	23	78
SN	8	4	7	3	24	16	6	20	88

Note: Seed regions-of-interest (ROIs) were categorized into seed-networks based on their location within our priori functional neurocognitive networks including default mode (DMN), frontoparietal (FPN) and salience network (SN). The number in the table represented the number of studies included in each SB-FC analysis of seed-networks in each of disorders. In an individual study, if several contrasts involved in the same seed-network, these contrasts were counted as one study.

Table S4. MNI Coordinates of Regions with Functional Connectivity Alterations within and between Neurocognitive Networks across Psychiatric Disorders.

Seed-network (and thresholding)	MNI coordinates	Maxstat.	Voxels	Description
DMN				
hb	2,40,-6	0.1465	900	Frontal_Med_Orb_R
	38,2,0	0.1328	488	Insula_R
	-6,-60,34	0.1291	173	Precuneus_L
	2,42,20	0.1241	93	Cingulate_Ant_L
	34,18,-16	0.1182	66	Insula_R
	0,-70,26	0.1140	48	Cuneus_L
	2,-58,22	0.1119	26	Precuneus_R
	2,-58,22	0.1114	23	Precuneus_R
	-6,20,-2	0.1078	19	Caudate_L
eb	2,24,2	0.1002	11655	Caudate_L
	-2,-60,30	0.1002	1662	Precuneus_L
FPN				
hb	-16,40,38	0.1488	9	Frontal_Sup_L
eb	-4,44,26	0.1345	1644	Frontal_Sup_Medial_L
	12,6,10	0.1315	483	Caudate_R
	46,16,8	0.1352	334	Frontal_Inf_Oper_R
SN				
hb	-38,8,-22	0.1641	93	Temporal_Pole_Sup_L
	-26,28,48	0.1532	63	Frontal_Mid_L
	-30,28,36	0.1479	24	Frontal_Mid_L
eb	-18,24,42	0.1349	1430	Frontal_Sup_L
	-40,10,-16	0.1349	1048	Insula_L
	26,8,-14	0.1292	741	Insula_R
	-2,46,6	0.1223	581	Cingulate_Ant_L

Table S5. Summary of Seed-Networks Included in SB-FC Meta-Analysis of Hypo- and Hyperconnectivity.

Networks	ADHD	ANX	ASD	BD	DPD	OCD	PTSD	SCZ	Total studies
DMN-hypoconnectivity	6	6	17	5	38	8	7	26	113
DMN-hyperconnectivity	4	7	12	3	23	9	6	18	82
FPN-hypoconnectivity	7	3	6	2	8	1	0	13	40
FPN-hyperconnectivity	4	2	8	2	9	3	0	10	38
SN-hypoconnectivity	3	2	4	1	18	10	2	12	52
SN-hyperconnectivity	5	2	3	2	6	6	4	8	36

Note: Seed regions-of-interest (ROIs) were categorized into seed-networks based on their location within our priori functional neurocognitive networks including default mode (DMN), frontoparietal (FPN) and salience network (SN). The number in the table represented the number of studies included in each SB-FC analysis of seed-networks in each of disorders. In an individual study, if several contrasts involved in the same seed-network, these contrasts were counted as one study.

Table S6. MNI Coordinates of Regions with Hypo- and Hyperconnectivity within and between Neurocognitive Networks across Psychiatric Disorders.

Seed-network (and thresholding)	MNI coordinates	Maxstat.	Voxels	Description
DMN: Patients < Controls				
hb	0,44,-8	0.1903	637	Frontal_Med_Orb_L
	-4,20,0	0.1536	141	Caudate_L
	-18,16,-2	0.1496	57	Putamen_L
eb	6,28,0	0.1275	7556	Caudate_R
	-40,6,-10	0.1262	982	Insula_L
	0,-58,28	0.1267	941	Precuneus_L
DMN: Patients > Controls				
hb	-40,32,-6	0.1639	21	Frontal_Inf_Orb_L
	42,-6,8	0.1632	16	Insula_R
	6,46,24	0.1628	14	Cingulate_Ant_R
	-40,24,-4	0.1670	12	Frontal_Inf_Orb_L
eb	-40,26,-4	0.1474	1229	Frontal_Inf_Orb_L
	38,2,2	0.1454	1037	Insula_R
	4,50,26	0.1469	786	Cingulate_Ant_R
	-6,-64,36	0.1382	736	Precuneus_L
	-36,32,30	0.1402	641	Frontal_Mid_L
FPN: Patients < Controls				
eb	8,4,14	0.1861	748	Caudate_R
FPN: Patients > Controls				
eb	-10,40,32	0.1900	552	Frontal_Sup_Medial_L
SN: Patients < Controls				
hb	-40,8,-20	0.2423	161	Temporal_Pole_Sup_L
eb	-40,10,-14	0.1926	1308	Insula_L
	-32,28,42	0.1889	779	Frontal_Mid_L
	48,14,38	0.1595	544	Frontal_Inf_Oper_R
	26,10,-8	0.1819	499	Putamen_R
	-2,36,18	0.1541	450	Cingulate_Ant_L
	-4,-58,28	0.1514	342	Precuneus_L
	44,-54,34	0.1778	277	Angular_R
SN: Patients > Controls				
eb	-48,-20,52	0.1795	496	Postcentral_L

Table S7. MNI Coordinates of Regions with Decreased Grey Matter across Psychiatric Disorders.

MNI coordinates	Maxstat.	Voxels	Description
Height-based threshold			
-42,28,-10	0.96	10355	Frontal_Inf_Orb_L
38,10,-2	0.83	5196	Insula_R
-58,-16,10	0.07	45	Temporal_Sup_L
Extent-based threshold			
40,20,-10	1.00	13832	Insula_R
2,44,14	1.00		Cingulate_Ant_R
-38,18,-16	1.00	12678	Insula_L
-2,50,2	1.00		Cingulate_Ant_L

Table S8. Distribution of Edges That Frequently Altered across Psychiatric disorders.

Networks	Hypoconnectivity	Hyperconnectivity
DMN-DMN	602	487
FPN-FPN	161	108
SN-SN	153	21
DMN-FPN	438	419
DMN-SN	468	317
FPN-SN	293	119
Interactions of other networks	1073	784

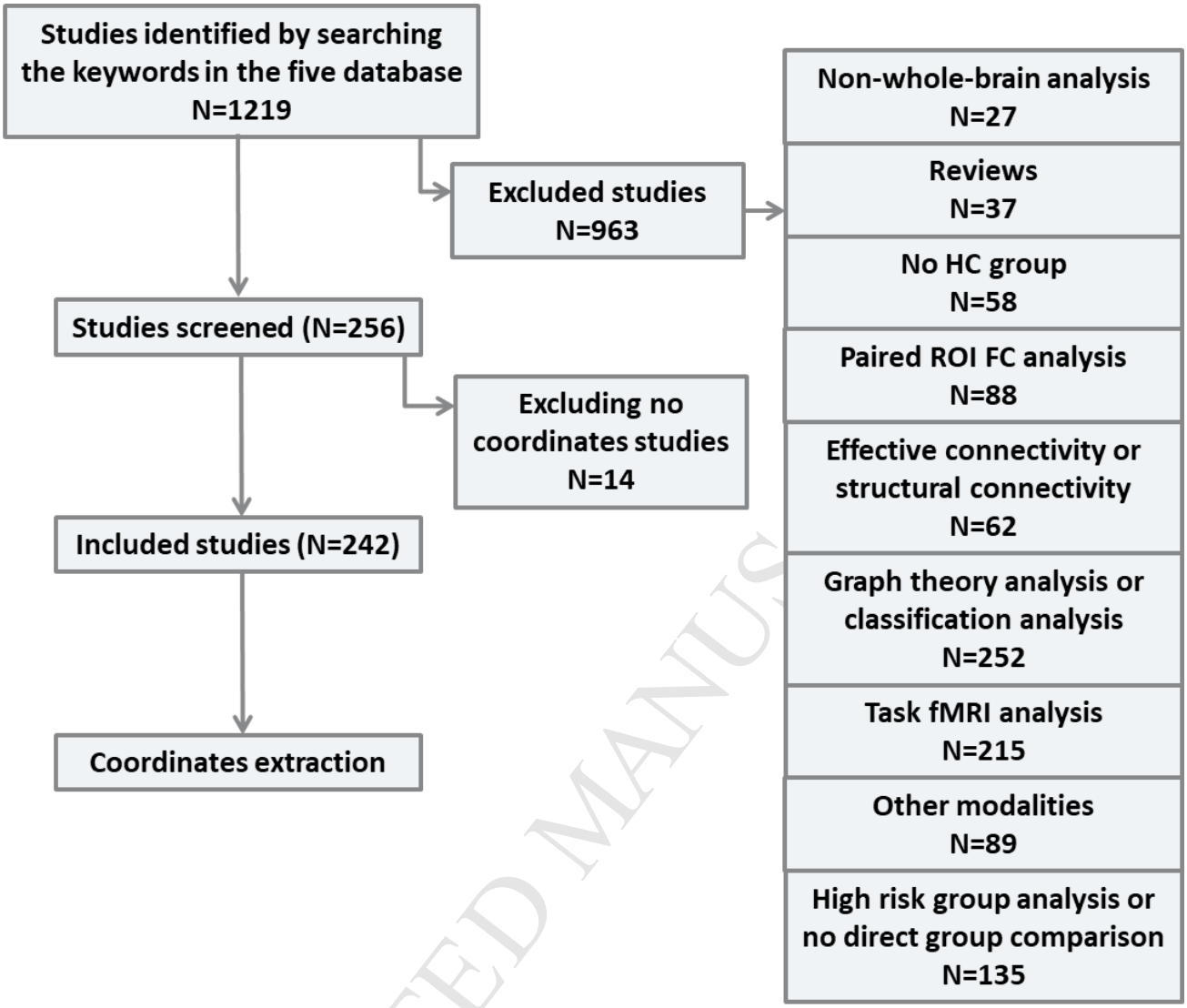

Figure S1. Flow Diagram of Study Selection in SB-FC Meta-Analysis.

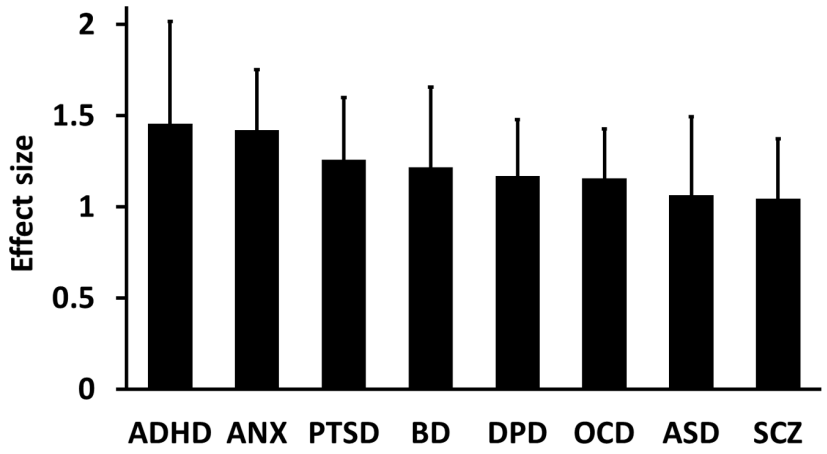

Figure S2. Effect Sizes Across Disorders in SB-FC Meta-Analysis.
Effect sizes were extracted from available 186 studies to calculate the mean and standard deviation values in individual disorder.

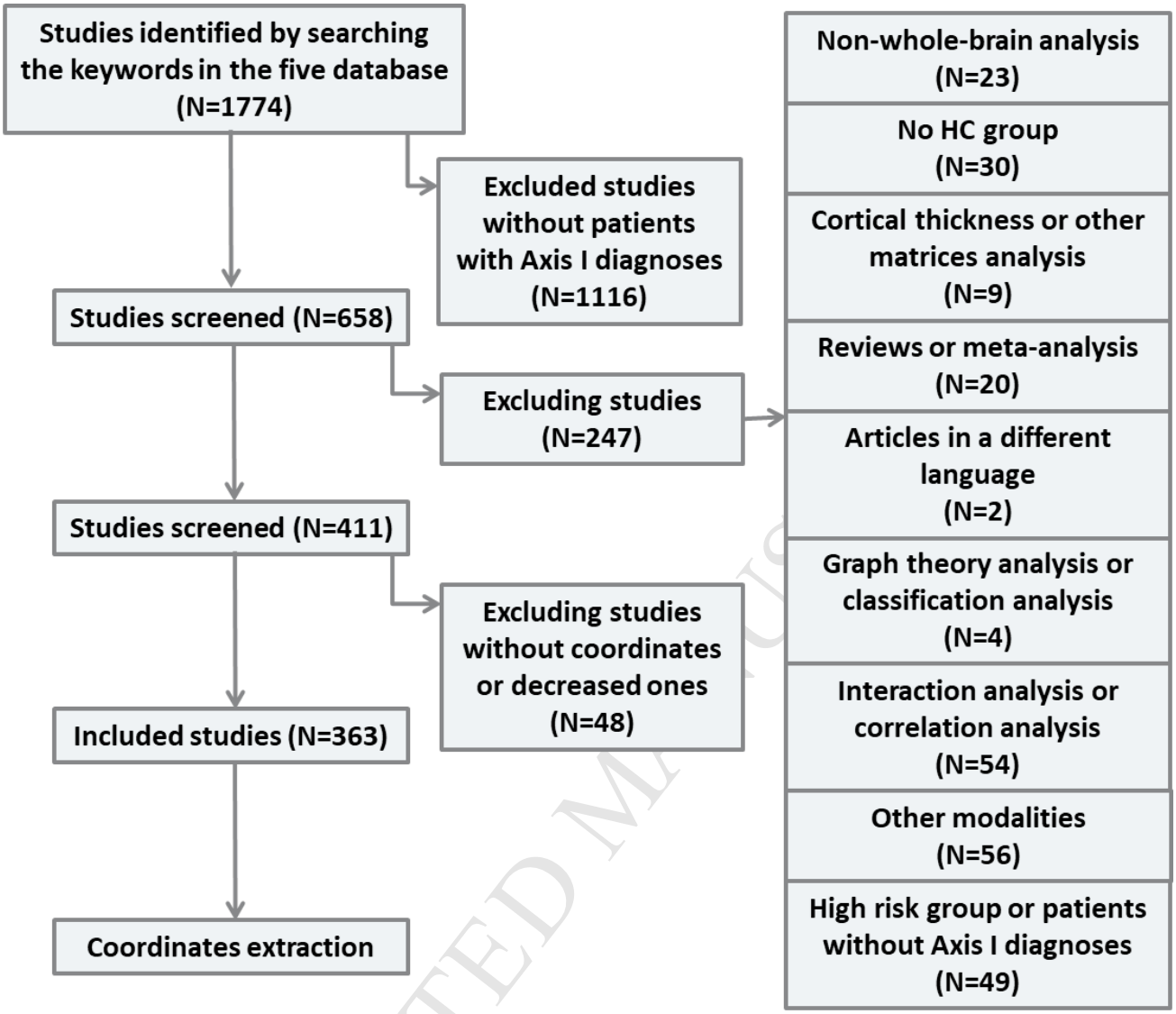

Figure S3. Flow Diagram of Study Selection in VBM Meta-Analysis.

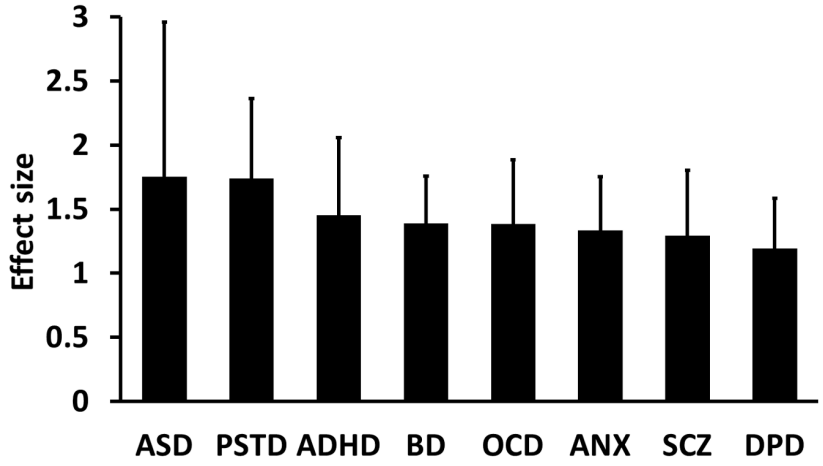

Figure S4. Effect Sizes Across Disorders in VBM Meta-Analysis.
Effect sizes were extracted from available 261 studies to calculate the mean and standard deviation values in individual disorder.

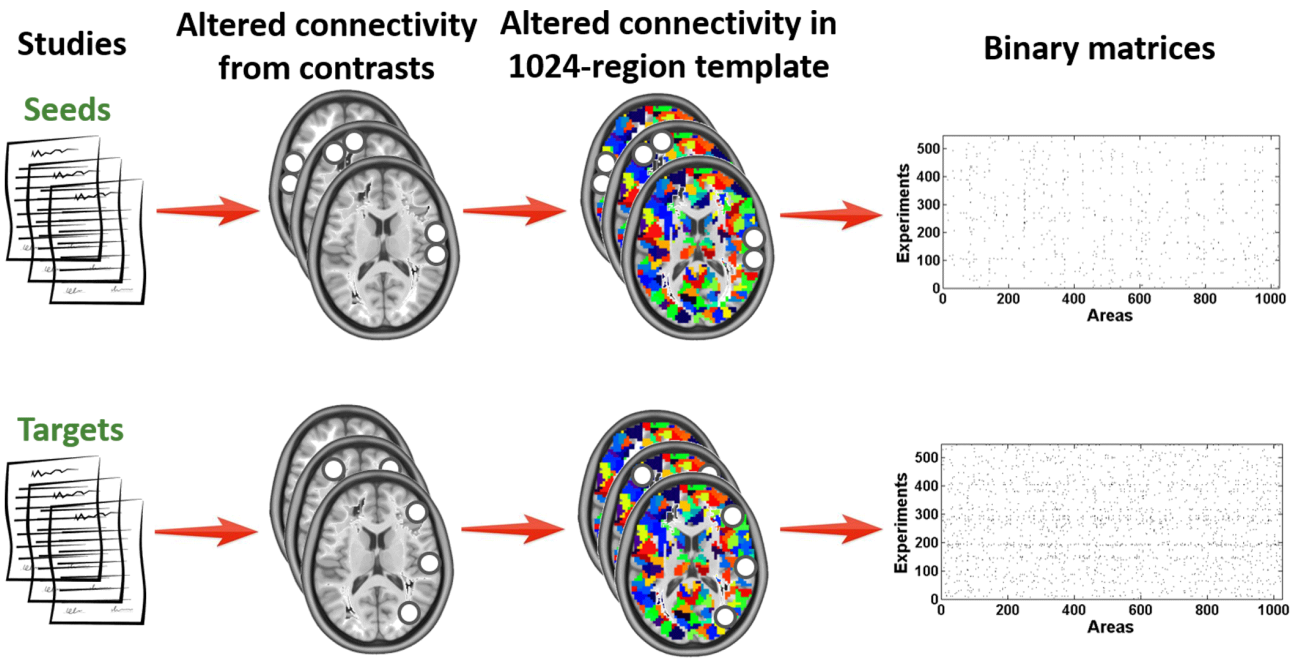

Figure S5. Constructing Network from the Meta-Analytic Dataset across Psychiatric Disorders.

We constructed separate SEED and TARGET binary networks. If a SEED or TARGET node was centered around its coordinates, then it was modeled as a 1 cm^3 sphere in a standard stereotactic space and aligned with the high-resolution 1024-region template. If a SEED node was a published anatomical mask, it was directed compared with the 1024-region template. The node was set to value of 1 if 20% or more of the SEED or TARGET nodes overlapped with the regional volume defined by the 1024-region parcellation template. Thus, for each contrast, we obtained the binary SEED and TARGET matrices. In each of the contrasts, an edge was defined as between the given SEED node and any of the TARGET nodes.

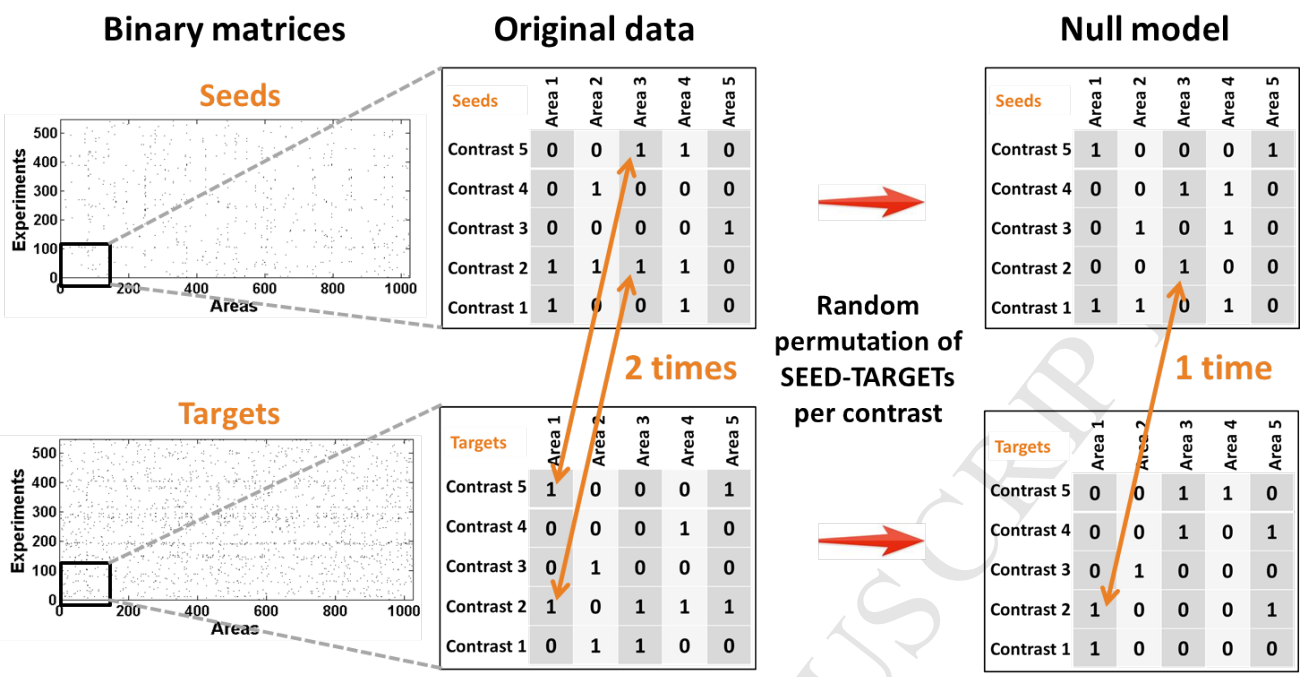

Figure S6. Consistently Altered Functional Connectivity Patterns across Psychiatric Disorders.

Columns represent different contrasts and rows areas. For each edge, we counted the frequencies of the edges that appeared to be altered across contrasts. Then, for each permutation, we randomly allocated SEED and TARGET nodes in each of the included contrasts and computed the frequencies of the edge across all the contrasts in a random model. The process was iterated 10,000 times and formed a null distribution. After NBS correction, we obtained a set of aberrant functional connectivity that frequently appeared across psychiatric disorders.

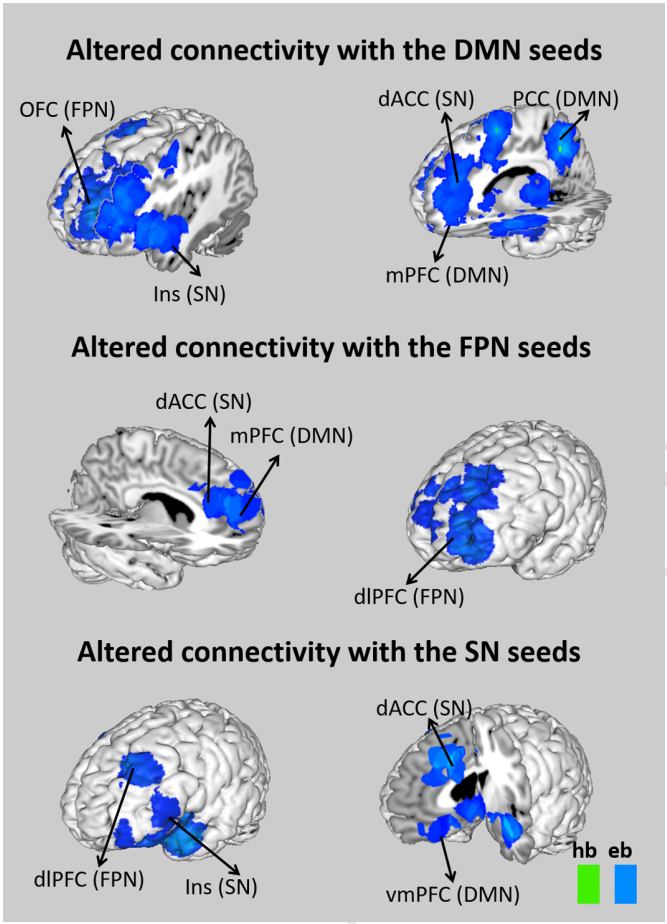

Figure S7. Functional Connectivity Meta-Analysis of Studies with Regression of Head Movement across Psychiatric Disorders.

The results showed aberrant communication within and between triple neurocognitive networks, which was similar patterns with the main findings. Abbreviations: DMN, default-mode network; FPN, frontoparietal network; SN, salience network; Cau, caudate; dACC, dorsal anterior cingulate cortex; dlPFC, dorsolateral prefrontal cortex; dmPFC, dorsomedial prefrontal cortex; Ins, insula; mPFC, medial prefrontal cortex; OFC, orbital frontal cortex; PCC, posterior cingulate cortex; TP, temporal pole; eb, extent-based threshold; hb, height-based threshold.

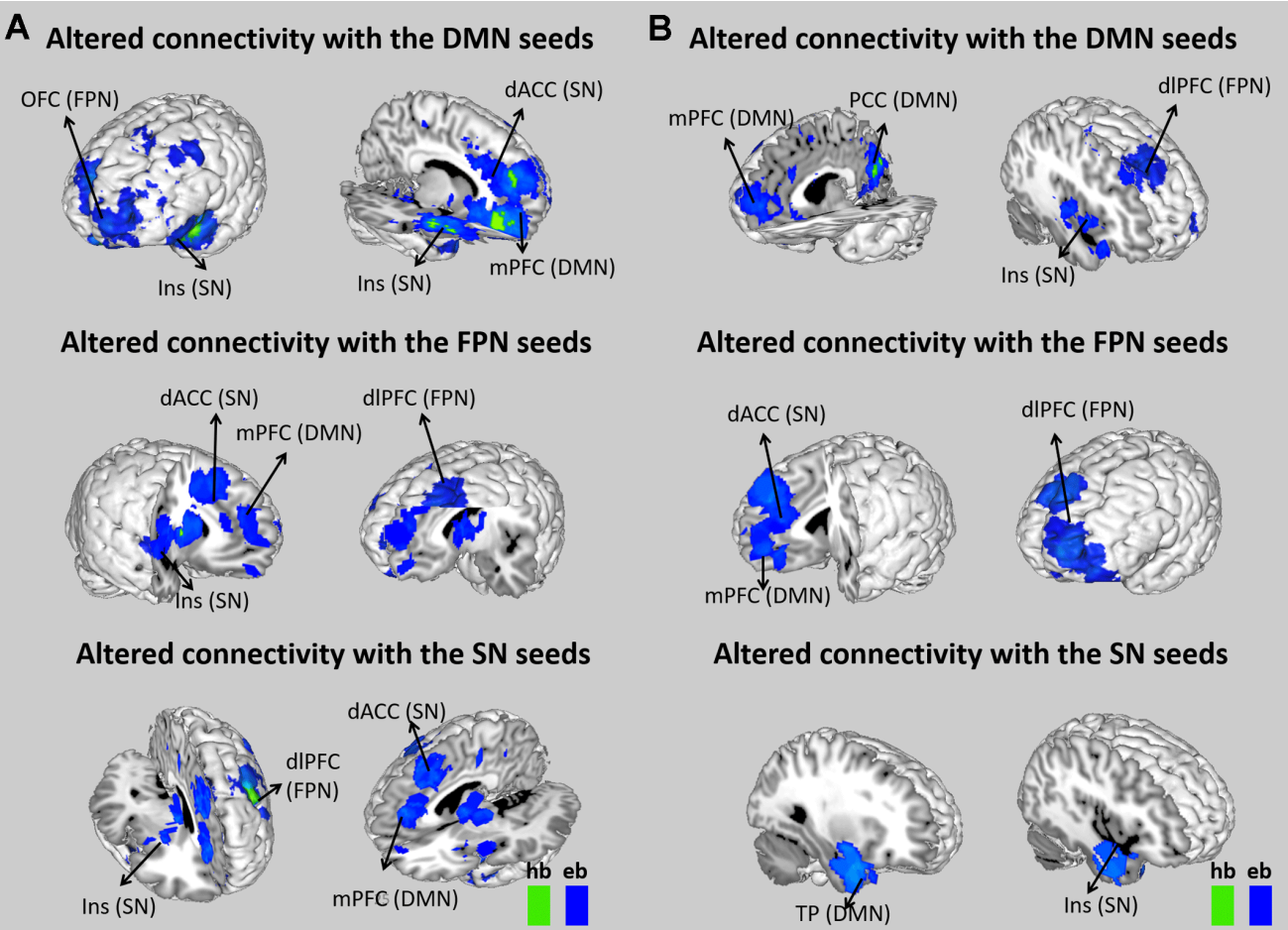

Figure S8. Functional Connectivity Meta-Analysis of Studies with and without GSR across Psychiatric Disorders.

(A) Meta-analytic results of altered functional connectivity patterns with triple neurocognitive networks by using the studies with GSR; (B) Meta-analytic results of altered functional connectivity patterns with triple neurocognitive networks by using the studies without GSR; Abbreviations: DMN, default-mode network; dACC, dorsal anterior cingulate cortex; dlPFC, dorsolateral prefrontal cortex; dmPFC, dorsomedial prefrontal cortex; Ins, insula; mPFC, medial prefrontal cortex; OFC, orbital frontal cortex; PCC, posterior cingulate cortex; TP, temporal pole; *eb*, extent-based threshold; *hb*, height-based threshold.

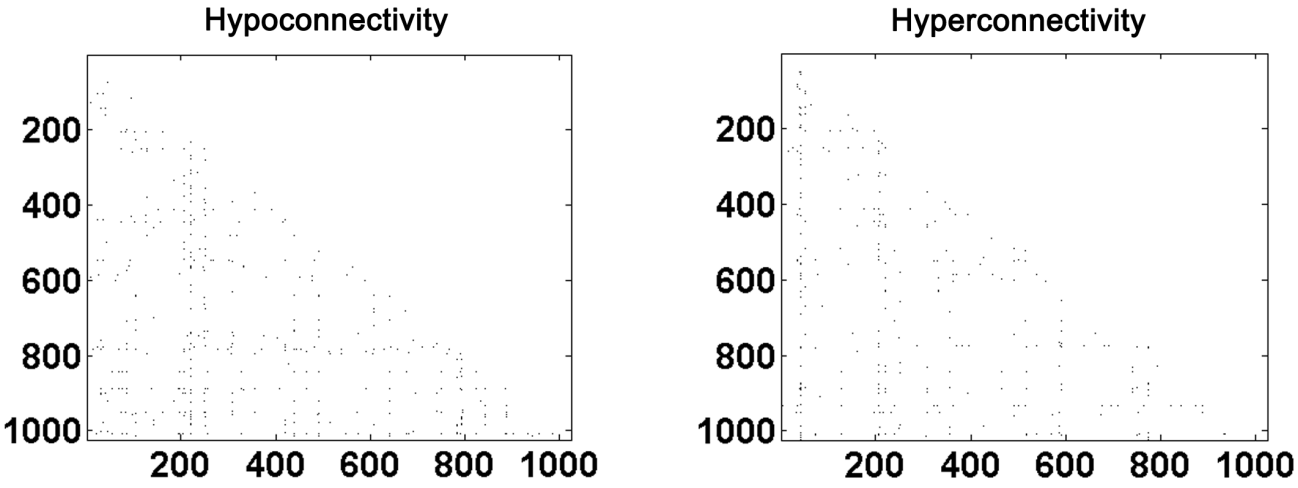

Figure S9. Significant Functional Hypo- and Hyperconnectivity across Psychiatric Disorders.

The result was a pattern of hypo- and hyperconnectivity that significantly appeared across psychiatric disorders in the 1024-region template.

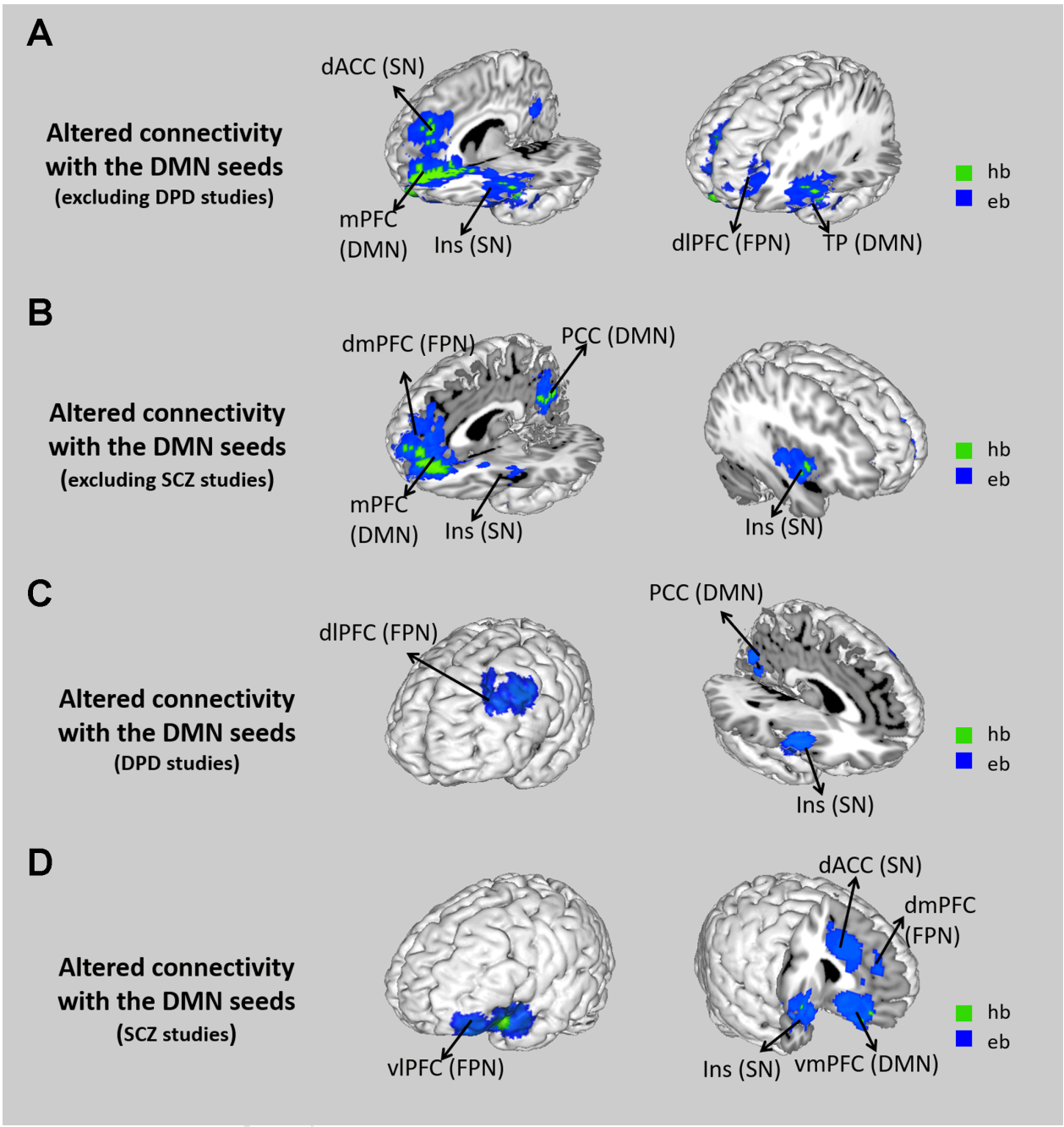

Figure S10. Functional Connectivity Meta-Analysis of Studies Excluding DPD and SCZ Studies.

(A) Altered connectivity patterns of DMN with the studies excluding of DPD; (B) Altered connectivity patterns of DMN with the studies excluding of SCZ; (C) Altered connectivity patterns of DMN with the studies of DPD; (D) Altered connectivity patterns of DMN with the studies of SCZ; Abbreviations: DMN, default-mode network; DPD, depression disorder; dACC, dorsal anterior cingulate cortex; dlPFC, dorsolateral prefrontal cortex; dmPFC, dorsomedial prefrontal cortex; Ins, insula; mPFC, medial prefrontal cortex; OFC, orbital frontal cortex; PCC, posterior cingulate cortex; TP, temporal pole; *eb*, extent-based threshold; *hb*, height-based threshold.

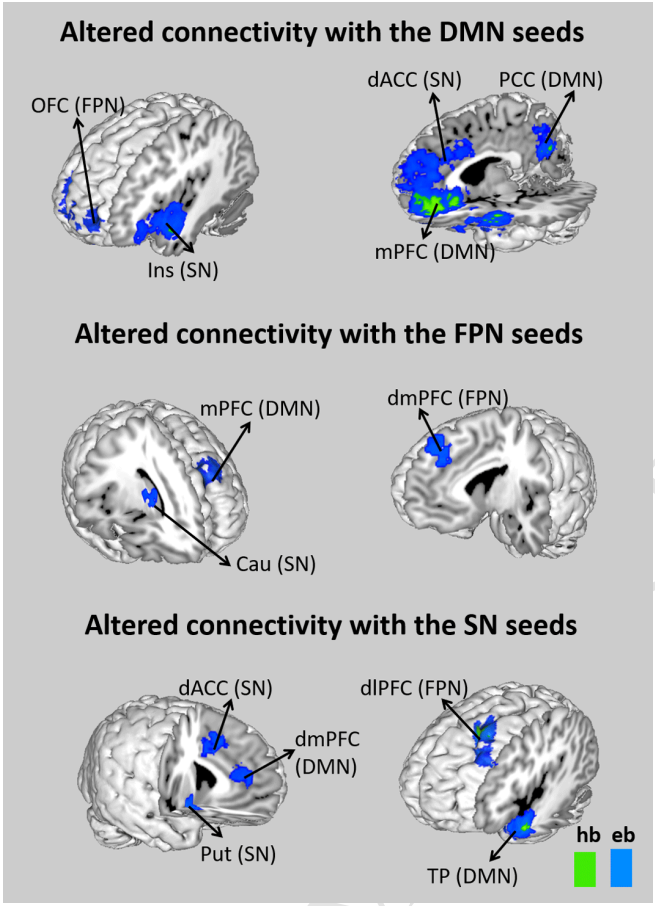

Figure S11. Functional Connectivity Meta-Analysis with 13mm as the Radius of Spherical Kernel.

The results showed aberrant communication within and between triple neurocognitive networks, which was similar patterns with the main findings. Abbreviations: DMN, default-mode network; FPN, frontoparietal network; SN, salience network; Cau, caudate; dACC, dorsal anterior cingulate cortex; dlPFC, dorsolateral prefrontal cortex; dmPFC, dorsomedial prefrontal cortex; Ins, insula; mPFC, medial prefrontal cortex; OFC, orbital frontal cortex; PCC, posterior cingulate cortex; TP, temporal pole; Put, putamen; eb, extent-based threshold; hb, height-based threshold.

Supplementary References

1. Sha Z, Xia M, Lin Q, Cao M, Tang Y, Xu K, et al. (2018): Meta-Connectomic Analysis Reveals Commonly Disrupted Functional Architectures in Network Modules and Connectors across Brain Disorders. Cereb Cortex. 28:4179-4194.
2. Menon V (2011): Large-scale brain networks and psychopathology: a unifying triple network model. Trends Cogn Sci. 15:483-506.
3. Zalesky A, Fornito A, Bullmore ET (2010): Network-based statistic: identifying differences in brain networks. Neuroimage. 53:1197-1207.
4. Glasser MF, Sotiropoulos SN, Wilson JA, Coalson TS, Fischl B, Andersson JL, et al. (2013): The minimal preprocessing pipelines for the Human Connectome Project. Neuroimage. 80:105-124.
5. Ugurbil K, Xu J, Auerbach EJ, Moeller S, Vu AT, Duarte-Carvajalino JM, et al. (2013): Pushing spatial and temporal resolution for functional and diffusion MRI in the Human Connectome Project. Neuroimage. 80:80-104.
6. Smith SM, Vidaurre D, Beckmann CF, Glasser MF, Jenkinson M, Miller KL, et al. (2013): Functional connectomics from resting-state fMRI. Trends Cogn Sci. 17:666-682.
7. Van Dijk KR, Sabuncu MR, Buckner RL (2012): The influence of head motion on intrinsic functional connectivity MRI. Neuroimage. 59:431-438.
8. Power JD, Barnes KA, Snyder AZ, Schlaggar BL, Petersen SE (2012): Spurious but systematic correlations in functional connectivity MRI networks arise from subject motion. Neuroimage. 59:2142-2154.
9. Murphy K, Fox MD (2017): Towards a consensus regarding global signal regression for resting state functional connectivity MRI. Neuroimage. 154:169-173.
10. Fox MD, Zhang D, Snyder AZ, Raichle ME (2009): The global signal and observed anticorrelated resting state brain networks. J Neurophysiol. 101:3270-3283.